

KARMA



Karst Aquifer Resources availability and quality in the **Mediterranean Area**

Tracer tests

Deliverable 2.4

Authors (in alphabetical order): Bartolomé Andreo Navarro (UMA), Juan Antonio Barberá Fornell (UMA), Marino Domenico Barberio (URO), Joanna Doummar (AUB), Nikolai Fahrmeier (KIT), Jaime Fernández Ortega (UMA), Simon Frank (KIT), Nadine Goeppert (KIT), Nico Goldscheider (KIT), Hervé Jourde (UM), Véronique Léonardi (UM), Valeria Lorenzi (URO), Marco Petitta (URO), Nataša Ravbar (ZRC SAZU), Vianney Sivelles (UM)

Date: August 2021



This project has received funding from the European Union's PRIMA research and innovation programme

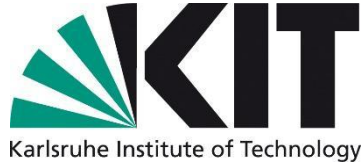




SAPIENZA
UNIVERSITÀ DI ROMA



Project Partners



(Coordinator)



SAPIENZA
UNIVERSITÀ DI ROMA



Executive Summary

Reliable information about transport processes in karst systems are essential to develop effective strategies for the management and protection of karst water resources. Tracer tests, combined with geological and hydrological observations are the most powerful method to delineate the catchment areas of karst springs, even in complicated geological and topographic settings. The delineation of spring catchments is crucial for the calculation of water budgets, which is especially important for the management of karst aquifers. For this reasons tracer tests are an important part of the KARMA project. Due to the worldwide pandemic, most of the initial planned field work could not be carried out as scheduled. Until mid-2021 just one new tracer test could be conducted in the Qachqouch aquifer in Lebanon. However, additional tests are planned for the remaining project time, e.g. in the Gran Sasso area (Italy).

Due to former research projects, tracer test results are already available for almost all KARMA test sites, including the Hochifen-Gottesacker system. Also, data from the Unica test site in Slovenia were added, where numerous tracer tests were conducted in the past decades. With the data from 111 tracer tests with 238 documented breakthroughs from five different field sites (Qachqouch aquifer, Málaga province Lez spring catchment, Hochifen-Gottesacker, Unica springs catchment) a comparison of distances, maximum velocities and peak velocities was made. The influence of known cave systems between injection and sampling point was also examined, as well as the effects of different hydrological conditions during the test period.

The tracer tests cover distances between 90 and 24,645 m, leading to a wide range of results. The comparison revealed a high variability of maximum flow velocities between 2.1 and 2,788 m/h. Also, tracer tests with a known cave system between injection and sampling point tend to show higher velocities than test without flow through a known cave system. The differentiation of the three flow conditions (low flow, mean flow, high flow) revealed an enormous impact on the tests results and especially on the documented velocities, with high flow leading to the fastest flow velocities. However, depending on the respective system and the degree of karstification, velocities can still be very low during high flow conditions.

Table of Contents

Technical References	1
Version History	1
Project Partners	1
Executive Summary	1
1. Introduction	3
1.1 Motivation	3
1.2 KARMA test sites for tracer tests	3
1.3 KARMA tracer test methodology	4
1.4 Innovative tracer test modelling approaches	5
1.5 Validation of vulnerability maps	5
1.6 References	6
2. Qachqouch aquifer (Lebanon)	7
2.1 Field site description	7
2.2 Tracer tests results	8
2.3 References	10
3. Málaga province (Spain)	11
3.1 Field site description	11
3.2 Graphical analysis of the BTCs	12
3.3 Solute transport modeling	14
3.4 Planned tracer test	15
3.5 References	15
4. Lez spring catchment (France)	16
4.1 Field site description	16
4.2 Tracer tests	17
4.3 References	21
5. Gran Sasso (Italy)	22
5.1 Field site description	22
5.2 Planned tracer tests	25
5.3 References	26
6. Hochifen-Gottesacker (Austria)	28
6.1 Field site description	28
6.2 Previous tracer tests	31
6.3 Planned tracer tests	35
6.4 Innovative Modeling	36

6.5	References	37
7.	Unica springs catchment (Slovenia)	38
7.1	Field site description	38
7.2	Tracer tests database	39
7.3	References	40
8.	Conclusions and outlook	42
8.1	General characteristics	42
8.2	Comparison of descriptive transport parameters	43
8.3	Impact of hydrological conditions	44
8.4	Tracer tests as tools for vulnerability assessment	44
8.5	References	45

1. Introduction

1.1 Motivation

Karst aquifers represent important water resources supplying many people with drinking water. However, these aquifers are highly vulnerable to contamination due to fast infiltration and the rapid transport of pollutants in karst conduits. Therefore, effective strategies for the management and protection of karst water resources must be based on reliable information about transport processes in the respective karst system.

Tracer tests, combined with geological and hydrological observations are the most powerful method to delineate the catchment areas of karst springs, even in complicated geological and topographic settings (Goldscheider et al., 2008). The delineation of spring catchments is crucial for the calculation of water budgets, which is especially important for the management of karst aquifers. Tracer tests can also provide information about the inaccessible parts of the conduit network in a karst aquifer, mainly in delimiting the active conduits that convey underground water between swallow holes, cave streams and springs. Tracer data, together with flow measurements, can also be used to estimate conduit cross-sectional areas and volumes, and to resolve conduit networks in more detail (Smart, 1988).

More advanced interpretation techniques allow the quantification of relevant contamination transport parameters, such as flow velocities, dispersivity, retardation and degradation as well as the characterization of conduit-matrix interaction (e.g. Geyer et al., 2007) and therefore tracer test results also represent an important input to WP3 (water quality, validation of vulnerability maps) and also for the calibration and validation of hydrological and hydrogeological models, tracer test data are important input parameters.

During the KARMA project, it was initially planned to cooperate strongly during the conduction of tracer tests. The tracer test(s) in the Italian Gran Sasso test site should be conducted in cooperation between KIT and URO. The alpine Hochifen-Gottesacker karst system was chosen as an additional test site.

1.2 KARMA test sites for tracer tests

In four KARMA test sites (Province Málaga, Lez catchment, Hochifen-Gottesacker, Qachqouch catchment) as well as in the Unica catchment numerous tracer test have been performed in the past (Fig. 1.1). The results of these tests can be used to compare the different field sites and examine variable behavior. Also new tracer tests are planned for several test sites.

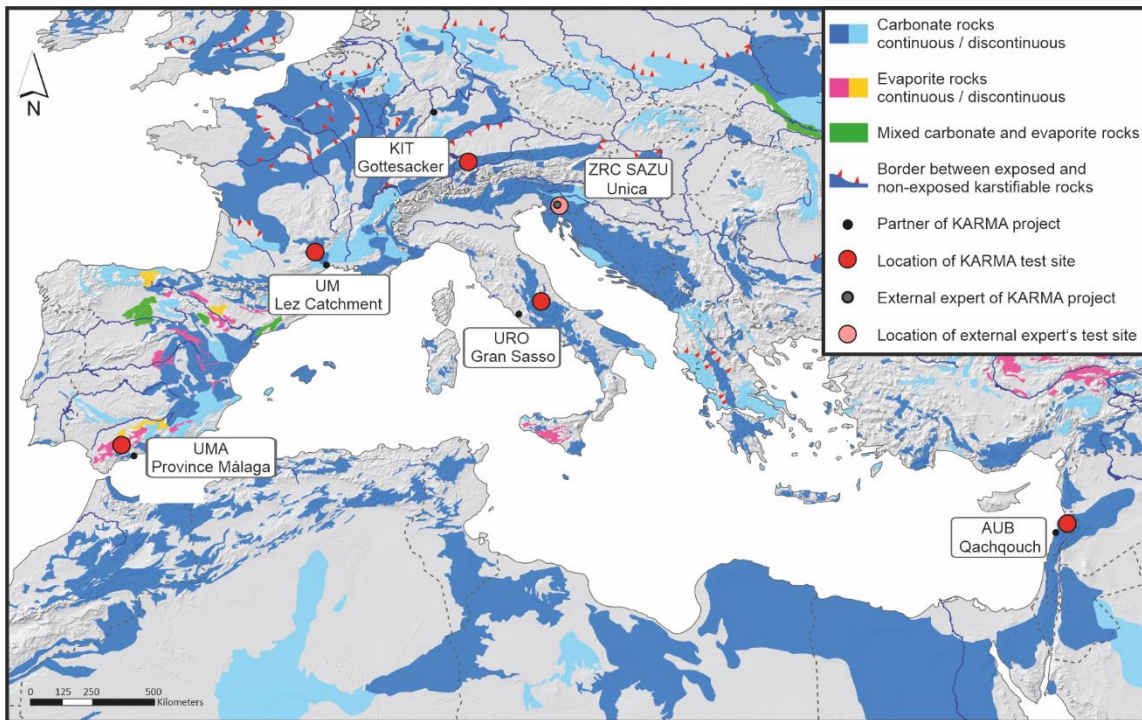


Fig. 1.1: Karst map of the Mediterranean region (detail from Chen et al. 2017) with the locations of the KARMA test sites where tracer tests were applied.

1.3 KARMA tracer test methodology

For the previous tracer tests in the KARMA test sites different kinds of tracers were used. Most tests were conducted with the fluorescence tracers Uranine, Eosine, Sulforhodamine B, Amidorhodamine G, Pyranine and Sodium-Naphthionate. Due to their low limits of detection and almost non-existent background concentrations, fluorescence tracers are usually the preferred choice. Additionally, Sodium Chloride and Lycopodium spores were used in the Unica springs catchment (Tab. 1.1).

Tab. 1.1: Overview of the tracers used in the individual test sites.

Tracer	Qachqouch aquifer	Malaga province	Lez spring catchment	Hochifen - Gottesacker	Unica springs catchment
Uranine	X	X	X	X	X
Eosine		X		X	
Sulforhodamine B		X	X	X	
Amidorhodamine G	X				X
Pyranine		X			
Sodium – Naphthionate	X				X
Sodium Chloride					X
Lycopodium spores					X

Tracer tests with fluorescence tracers are usually monitored with the help of water samples from the sampling points, usually springs, which are then analyzed in a laboratory to gain tracer concentrations and from them a breakthrough curve, a series of concentration-time data (Goldscheider et al., 2008). A higher temporal resolution of the breakthrough curve can be obtained by the use of a mobile field fluorimeter at the most important sampling points (Schneegg & Flynn, 2003).

With a breakthrough curve transit times and velocities can be determined (Fig. 1.2). With the time of the first detection (t_1) and the distance between injection and sampling point, the maximum velocity can be calculated. The peak time (t_p , time of maximum concentration) results in the dominant velocity.

If the discharge at the sampling point is monitored during the test, recovery rates can be calculated, which allow a further interpretation of the results. With the time of half recovery ($t(R/2)$) for the respective sampling point, the mean velocity can be determined (Goldscheider et al., 2008).

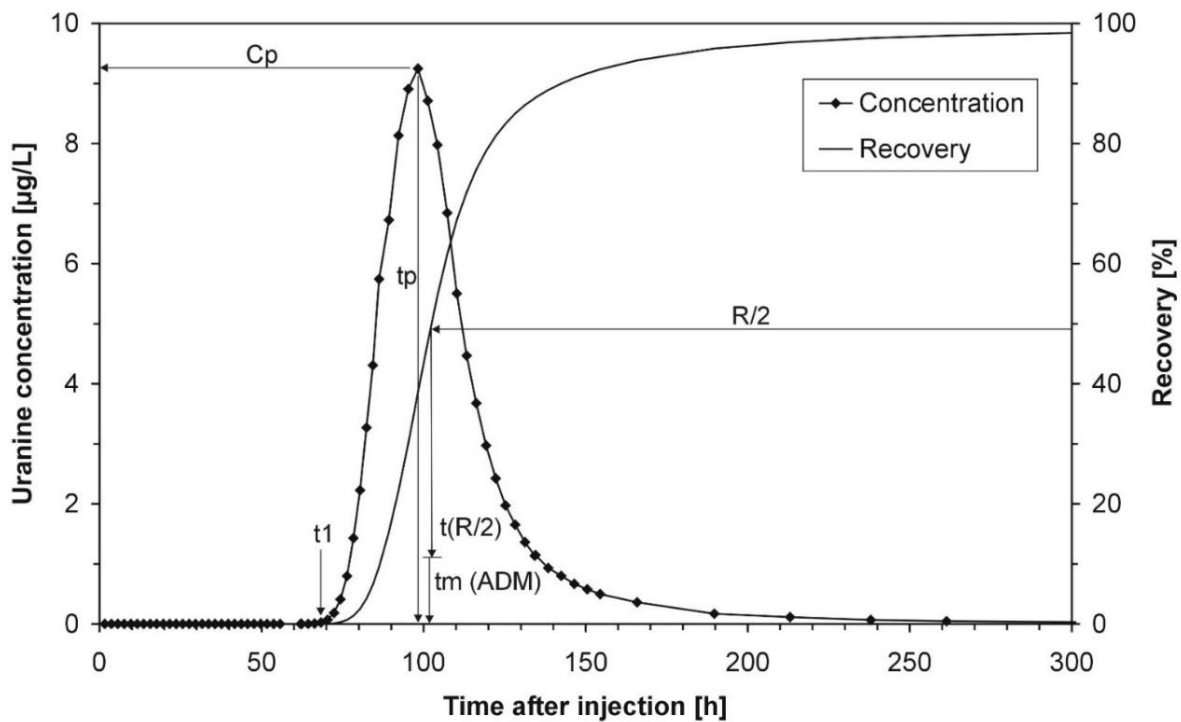


Fig. 1.2: Example of a breakthrough curve and the parameters that can be derived from it: t_1 (time of first detection), t_p (time of maximum concentration), C_p (maximum concentration), $t(R/2)$ (time of half recovery) (Goldscheider et al., 2008).

1.4 Innovative tracer test modelling approaches

To obtain transport parameters, especially as preparation for potential contaminations, breakthrough curves are usually modeled using either an ADM (advection-dispersion model) or a 2RNE model (two-region nonequilibrium model). The commonly used ADM inverts the general advection-dispersion equation (Kreft & Zuber, 1978) and fits a modeled breakthrough curve to observed values, leading to an estimation of flow parameters (Lauber et al., 2014). Additionally, 2RNE models consider the exchange between mobile and immobile fluid region by extending the advection-dispersion equation (Field & Pinsky, 2000). Immobile fluid zones are assumed as stagnant compared to the water in mobile regions.

The new CTRW (continuous time random walk) approach improves the fitting of long-tailed breakthrough curves. The physically-based and probabilistic CTRW can describe non-Fickian flow and allows modeling and interpretation of tracer data from various geological settings, since it can include ADM, 2RNE and several additional multirate and time-fractional approaches (Berkowitz et al., 2006; Goeppert et al., 2020).

1.5 Validation of vulnerability maps

Vulnerability maps with respect to karst groundwater quality are an important tool for a better and precise groundwater protection and are highly requested by local water authorities and National Park services in the KARMA test sites. As one task of the KARMA project, vulnerability maps will be created for each site using the COP method (Daly et al. 2002; Andreo et al., 2006), in order to identify areas

with a high contamination risk. As a link between WP2 and WP3, the vulnerability maps will demand a validation procedure by applying tracer tests in order to assess the different vulnerability classes.

1.6 References

- Andreo, B., Goldscheider, N., Vadillo, I., Vias, J.M., Neukum, C., Sinreich, M., Jimenez, P., Brechenmacher, J., Carrasco, F., Hötzl, H., Perles, J.M., Zwahlen, F. (2006) Karst groundwater protection: First application of a Pan-European Approach to vulnerability, hazard and risk mapping in the Sierra de Libar (Southern Spain), *Science of the Total Environment*, 357, 1-3, 54-73.
- Berkowitz, B., Cortis, A., Dentz, M., Scher, H. (2006) Modeling non-Fickian transport in geological formations as a continuous time random walk, *Reviews of Geophysics*, 44, 2, 1-49.
- Daly, D., Dassargues, A., Drew, D., Dunne, S., Goldscheider, N., Neale, S., Popescu, I., Zwahlen, F. (2002) Main concepts of the „European approach“ to karst-groundwater-vulnerability assessment and mapping, *Hydrogeology Journal*, 10, 340-345.
- Field, M.S., Pinsky, P.F. (2000) A two-region nonequilibrium model for solute transport in solution conduits in karstic aquifers, *Journal of Contaminant Hydrology*, 44, 3-4, 329-351.
- Frank, S., Goepfert, N., Goldscheider, N. (2021) Field Tracer Tests to Evaluate Transport Properties of Tryptophan and Humic Acid in Karst, *Groundwater*, 59, 1, 59-70.
- Geyer, T., Birk, S., Licha, T., Liedl, R., Sauter, M. (2007) Multitracer Test Approach to Characterize Reactive Transport in Karst Aquifers, *Groundwater*, 45, 1, 36-45.
- Goepfert, N., Goldscheider, N., Berkowitz, B. (2020) Experimental and modeling evidence of kilometer-scale anomalous tracer transport in an alpine karst aquifer, *Water Research*, 178.
- Goldscheider, N., Meimann, J., Pronk, M., Smart, C. (2008) Tracer tests in karst hydrogeology and speleology, *International Journal of Speleology*, 37, 1, 27-40.
- Kreft, A., Zuber, A. (1978) On the physical meaning of the dispersion equation and its solution for different initial and boundary conditions, *Chemical Engineering Science*, 33, 1471-1480.
- Lauber, U., Ufrecht, W., Goldscheider, N. (2014) Spatially resolved information on karst conduit flow from in-cave dye tracing, *Hydrology and Earth System Sciences*, 18, 435-445.
- Schnegg, P.A., Flynn, R. (2003) Online Field Fluorometers for hydrogeological tracer tests, *Wissenschaftliche Mitteilungen, Institut für Geologie, Technische Universität Bergakademie Freiberg*.
- Smart, C.C. (1988) Artificial Tracer Techniques for the Determination of the Structure of Conduit Aquifers, *Groundwater*, 26, 4, 445-453.

2. Qachqouch aquifer (Lebanon)

2.1 Field site description

Qachqouch Spring is located in the Metn area in Lebanon; 18 km north from Beirut, draining a catchment that has been delineated by water balance and numerical model to be about 56 km² (Dubois et al., 2020). It originates from the Jurassic karst aquifer (J4) and discharges from the Upper Jurassic Formation (J6; Walley, 1997), at about 64 meters above sea level (Fig. 2.1). The Jurassic formation is mainly formed of limestone; with intertonguing dolostones in the lower parts of the formation because of diagenetic dolomitization (Nader et al., 2004). The Jurassic massive limestone is often marked by karstification, but there are no known large infiltration zones (Hahne, 2011).

During low flow periods, the spring is used during water shortages in Beirut and surrounding areas. The total yearly discharge of Spring Qachqouch reaches 60 Mm³ based on high resolution monitoring of the spring (2014-2017). The discharge maximum recorded at Qachqouch Spring reaches 10 m³/s for a short period of time following flood events. It's about 2 m³/s during high flow periods and 0.2 m³/s during recession. The total yearly precipitation is estimated to be 1000 mm on average, from one station deployed in the Qachqouch catchment at 950 m asl and one station at 1700 m in the area upstream of the direct catchment (2014-2017 local high-resolution monitoring).

High resolution analyses of hydrographs and climatic data show that the Qachqouch karstic system has both transmissive and capacitive functions (Dubois et al., 2020). The system has been conceptualized by three different reservoirs emptying into each other to model the recessions and depletions. The model shows a quick response function which makes the Spring reactive to rain events; and that is linked to fractured conduits that allow fast flow. A relatively slower reservoir, which is activated during the rainy season in between events, is probably linked to crushed limestone associated with dolomite. A third and large storage reservoir, which along with the epikarst, gives the Spring a capacitive behavior and keeps it flowing in a depletion state during summer/dry seasons.

Nahr El Kalb River originates from Nabaa El Assal and Laban springs in the highlands of Kesrouane (Faraya-Sannine), in addition to interflow and runoff occurring shortly after rain events. Its catchment extends from the outlet of the River on the coast to about 22 km to the east in the Lebanese Mountains. Its southern and northern boundaries were delineated on topographic highs. The river consists of three sub-catchments (RI -Nahr El Salib; RII-Nahr el Ouadi, and RIII- Nahr Abou Mizane) joining together to form the main branch of the River (Fig. 2.1).

Its discharge may exceed a maximum of 22 m³/s, whereas it runs dry during low flow periods, (from July-September of the hydrogeological year) with a total discharge yearly volume of 80-230 Mm³ (Data from the Litani Water Authority).

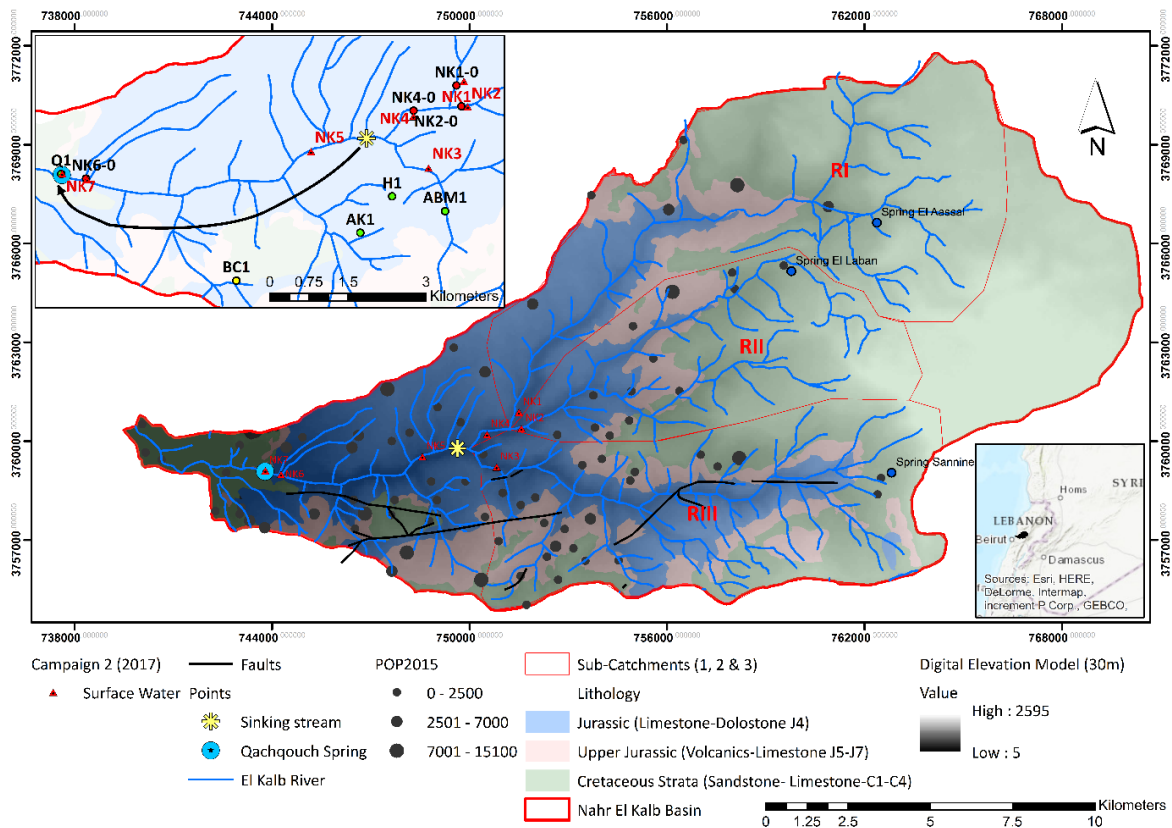


Fig. 2.1: Geological map showing the Qachqouch spring within the watershed of Nahr El Kalb River and the approximate location of the sinking stream (Doummar and Aoun, 2018a)

Qachqouch spring is highly polluted due to excessive waste discharge located in its urbanized catchment upstream. Raw wastewater is either directly discharged into the river system or stored on the catchment in bottomless septic pits or abandoned boreholes, as there are no effective wastewater treatment plants in the catchment area. Other sources of pollution include a poultry farm, solid waste dumps, hospitals, and quarries discharging their effluents into the River, thus posing a threat to the Qachqouch spring. Therefore, the tracer injection was done in the River and monitored at the Spring.

2.2 Tracer tests results

Qachqouch Spring is about 100 meters downside of the Jeita Spring. Twenty-four tracer tests within the framework of a project funded by the BGR conducted on the Jeita Spring revealed that there is no connection between its catchment located north of Nahr El Kalb River and Qachqouch Spring, showing that each of the two springs are independent (Doummar et al., 2018a). These tracer experiments allowed the estimation of transport, mean velocities and longitudinal dispersivities in different compartments of the karst system (Doummar et al., 2018a), revealing relatively low transit times reflective of a mature karst system. Additionally, tracer experiments were undertaken on the upper catchments drained by the two springs forming the El Kalb River.

The four tracer tests were undertaken to determine a hydrogeological connection between Qachqouch Spring and Nahr el Kalb sinking stream, and to quantify the connection (Aoun, 2019). Uranine (sodium fluorescein) and occasionally Amidorhodamine-G were used as they are considered non-toxic to humans, animals and the environment, and conservative (Käss, 1998).

Four artificial tracer tests were conducted in Mar/2016, Feb/2017, Nov/2017, and the last one in June/2020 as part of the KARMA project. The injection was instantaneous and the injection point of the tracer tests was about 8900 m from the Qachqouch Spring, a few hundred meters before the sinking stream. The injection time was noted and tracer concentrations were simultaneously monitored in the spring using a field fluorometer (GGUN-FL30; Schnegg, 2002) that was calibrated for the applied tracers. The fluorometer measures and stores dye concentrations at the monitoring site at specific time intervals (every 15 min).

The tracer breakthrough curve (BTC) recorded at the Qachqouch spring reveals a connection between the River and the spring (Fig. 2.1 and Fig. 2.2). The breakthrough curves were characterized by one main peak and other minor peaks or discontinuous recovery of the tracer for a longer period. The injected dye was first detected at the spring between 5 to 20 hours after injection, which corresponds to maximum transport velocities of 0.07 m/s, 0.17 m/s, 0.25 m/s, and 0.77 m/s in, May, November, June, and February respectively (Aoun, 2019, Doummar et al., in review; Fig. 2.2). The mean velocities and dispersivities are estimated for the first main peak of the BTC based on 1-D analytical solutions for transport Advection Dispersion model (ADM) and the Two-Region Non-equilibrium model (2RNE) depending on the extent of tailing and shape of the BTC (Fig. 2.2). The dispersivities ranging between 39 and 780 m are indicative of transport in karst (Doummar et al., 2018a).

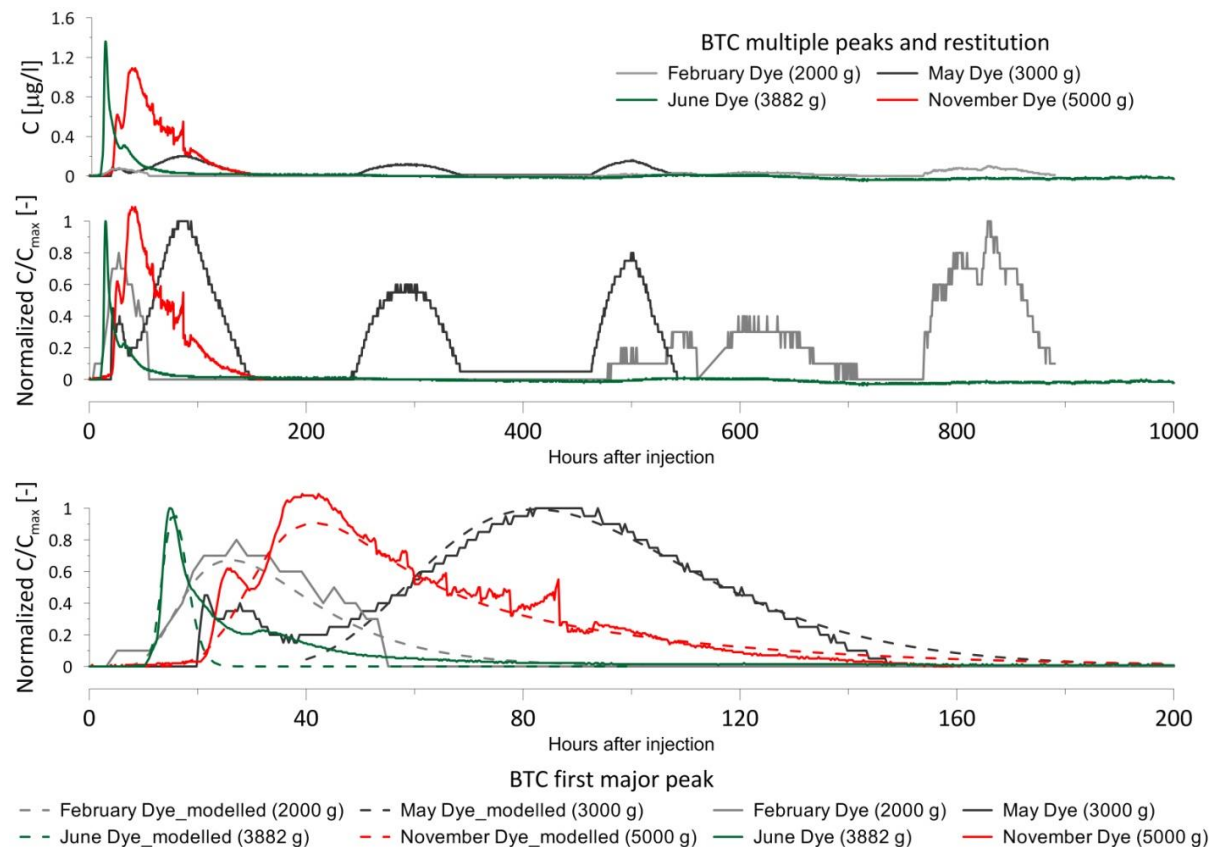


Fig. 2.2: Tracer breakthrough curves (BTC) recorded at Qachqouch springs from four injections in the Nahr El Kalb sinking stream (2016-2020). First peaks in the BTCs are modelled using 2RNE model to account for the tailing effect (Doummar et al., in review).

The tracer experiment indicates a relationship between the heavily polluted River and the spring under different flow conditions. During high flow conditions, as the base level in the River is higher, infiltration through fast flow pathways along the river (sinking streams) is more prominent, as indicated by the higher mass recovery during February (8 % compared to 1 % during the lowest flow). The first peak in the BTC recovered in the Qachqouch lasts between 2.5-6.5 days, while the tracer

continues to appear in the spring for more than 40 days. The multi-peak BTC shows that the River and the Spring are linked by continuous infiltration or through multiple conduits or multiple sinking streams. Additionally, another tracer test is planned later this year in a doline in the catchment area to confirm the hydrogeological connection between the area south of the Nahr El Kalb River and calculate transport parameters in the subsurface from a preferential infiltration point to the Qachqouch spring.

2.3 References

Aoun, M.: Occurrence and Transport of selected Micropollutants in Surface water and Groundwater under varying dynamic conditions: Application on the Qachqouch karst catchment Lebanon. Master thesis, American University of Beirut, Department of Geology, Beirut, Lebanon. 2019

Doummar, J. and Aoun, M.: Occurrence of selected domestic and hospital emerging micropollutants on a rural surface water basin linked to a groundwater karst catchment, *Environmental Earth Sciences*, 77(9), 351, doi: 10.1007/s12665-018-7536-x, 2018b.

Doummar, J., Fahs M., Aoun M., ElGhawi, R., Othman, J., Alali, M., and Kassem A., H. (2021) Assessment of water quality and quantity of springs at a pilot-scale: Applications in semi-arid Mediterranean areas in Lebanon. Threats on Springs. In review.

Doummar, J., Margane, A., Geyer, T., and M. Sauter (2018a) Assessment of key transport parameters in a karst system under different dynamic conditions based on tracer experiments: the Jeita karst system, Lebanon. *Hydrogeol J.*, doi.org/10.1007/s10040-018-1754-x

Dubois E., Doummar J., Pistre S., Larocque M. Calibration of a semi-distributed lumped model of a karst system using time series data analysis: the example of the Qachqouch karst spring. *Hydrol. Earth Syst. Sci.*, 24, 4275–4290, doi.org/10.5194/hess-24-4275-2020, 2020.

Hahne, K., Abi Rizk, J., and Margane, A. Geological Map of the Jeita Groundwater Contribution Zone. - German-Lebanese Technical Cooperation Project Protection of Jeita Spring, Technical Report. Raifoun. 2011

Käp W (1998) Tracing technique in geohydrology. Balkema, Rotterdam, The Netherlands, 589 pp

Nader, F. H, and Swennen, R. The hydrocarbon potential of Lebanon: New insights from regional correlations and studies of Jurassic Dolomitization. *JPG Journal of Petroleum Geology* 27, no 3: 253 75, 2004.

Schnegg, PA (2002), An inexpensive field fluorometer for hydrogeological tracer tests with three tracers and turbidity measurement. In: Bocanegra E, Martinez D, Massone H (ed) Proc. of the XXX/IAH Congress Groundwater and Human Development. Mar Del Plata, Argentina, October 2002, 1484–1488

3. Málaga province (Spain)

3.1 Field site description

Six mountainous karst systems in Malaga province (southern Spain) were investigated through field tracer tests methods between 2009 and 2015, resulting in 15 tracer breakthrough curves (BTCs) (Barberá et al., 2018) (Fig. 3.1): Villanueva del Rosario, Los Tajos, Hidalga-Turón, Fuensanta Valley, Jarastepar massif and Utrera. All test sites present common features such as elevations ranging from 100 to 1,650 m above sea level (asl) and are characterized by rainfall events which present a strong seasonal pattern in the annual distribution of precipitation; thus, rainfall mainly occurs in autumn, winter and (to a lesser extent) in spring seasons.

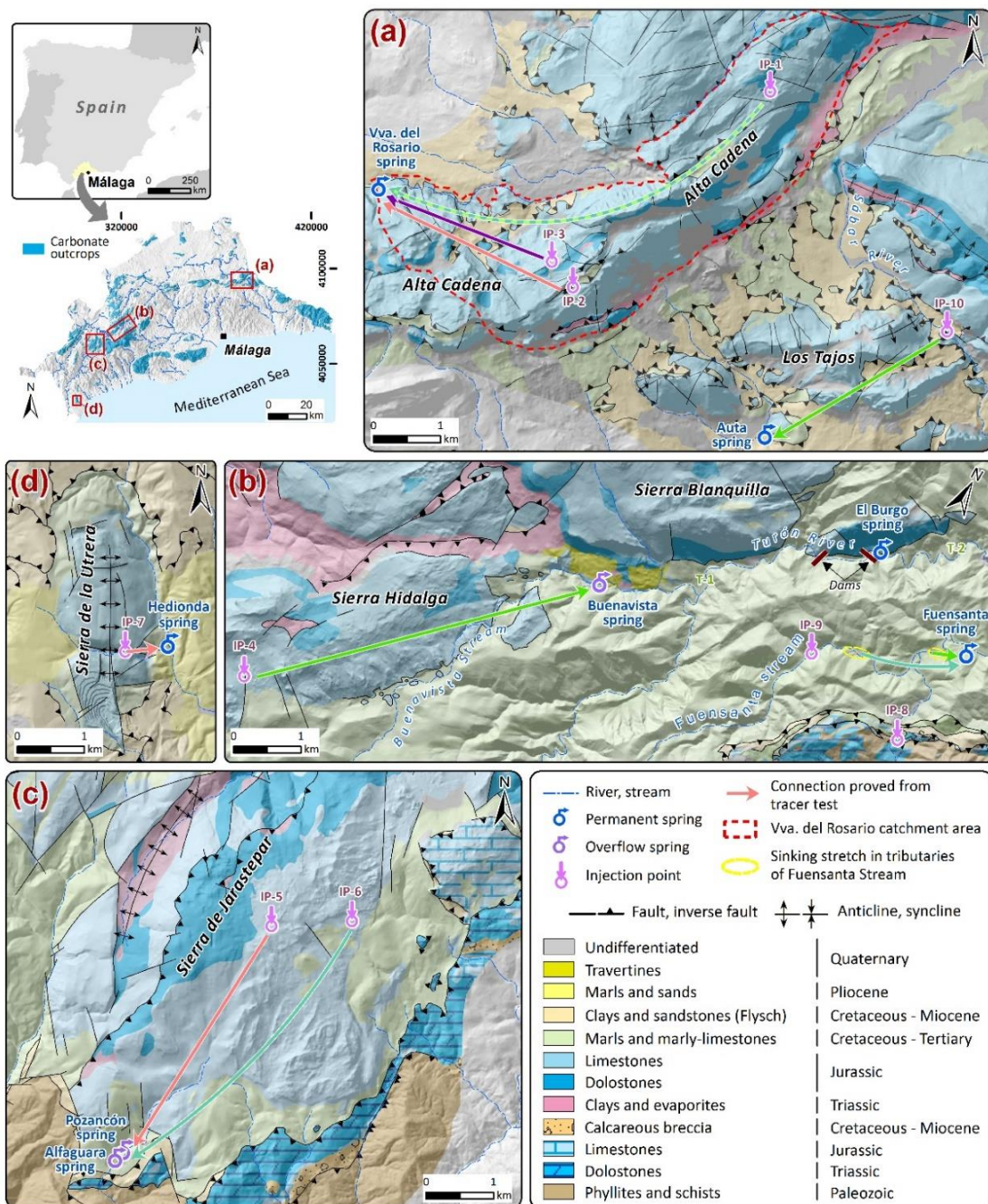


Fig. 3.1: Location (regional context and detailed spatial information) and geological and hydrogeological characteristics of the study sites. Karst flow paths and injection and sampling points are also shown. (taken from Barberá et al., 2018).

The geological structure is complex due to the deformation processes produced by the collision between Internal and External zones of the Betic alpine orogen. Almost all systems (except for Cretaceous–Tertiary marls and marly-limestones formation of Fuensanta Valley) consist of 450–550 m thick, folded and fractured Jurassic dolostones and limestones (Fig. 3.1). The carbonate aquifers are enveloped by Upper Triassic clays and evaporites (at the bottom) and Lower Cretaceous–Oligocene marly limestones and marls (at the top), while Neogene flysch-type clays and sandstones generally overthrust the entire Mesozoic rock sequence (Martín-Algarra 1987). Previous investigations have proven the development of secondary porosity and permeability through fissuration and/or karstification processes, which grant a particular hydrogeological heterogeneity to Jurassic carbonate formations (Barberá et al. 2012; Mudarra et al. 2012, 2014; Barberá and Andreo 2015, 2017; De la Torre et al. 2017).

Recharge processes at the different test sites mainly occurs by direct infiltration of rainwater through carbonate outcrops, but also by concentrated infiltration through sink holes or induced recharge due to allogenic runoff produced in adjoining low-permeability materials. Groundwater discharge is produced through springs usually located at the contact between carbonate formations and impervious layers (in the case of Fuensanta Valley, through an outlet draining Cretaceous marls and marly-limestones) (Barberá et al., 2018). Pozancon, Buenavista and Alfaguara springs drain groundwater only during flooding episodes.

3.2 Graphical analysis of the BTCs

Due to the fact that different injection points exist and discharge is not produced at only one outlet in some of the test sites, 15 BTCs (Fig. 3.2) were obtained and easily identifiable. The BTCs were recorded using PERKIN ELMER LS55 laboratory luminescent spectrometer for sample analysis and also GGUN FL-30 was used in the field for three of the tracer tests. The different hydrological conditions in which the experiments were performed and the diverse transport dynamics features of individual traced flow paths are reflected in the varied curve shapes and magnitudes of the obtained BTCs. Linear distances between injection and sampling points range from 2100 m (BTC13) to 10600 m (BTC7), aside from Hedionda system tracer test, which distance between both points is 605 m (BTC12).

As it can be seen on Figure 2, the BTC curves which display narrow and peaky shapes correspond to tracing experiments realized under high or high-intermediate flow conditions (BTC1 to BTC11). However, in the tracer tests carried out when no recharge is produced (intermediate-low flow conditions), the obtained BTCs generally show smoother and wider shapes with long tails (BTC13, BTC15). The travel time of first dye detection and peak concentration were minimum in BTC4 (12.1–14.1 h) and maximum in BTC15 (120–183 h). As a general rule, the time lag between these two key points of the examined BTCs was 11.9 h, maximum peak concentration was measured in BTC5 (258.9 µg/l of URN) and the minimum one in BTC15 (0.46 µg/l of URN) (Barberá et al., 2018). The duration of the breakthrough curves also displays a high variability depending on the investigated system and range from 0.87–12.04 days (BTC10 and BTC5) to 18.42–33.29 days (BTC12 and BTC14).

The recovery rates of the injected tracers were higher in the experiments performed under high flow (e.g. 60% for URN in BTC1 and 91.9% for PYR in BTC11). On the other hand, the lowest recovery rates (<10%) were obtained for those tracer tests in which the injection was realized through sinking river stretches under intermediate–low flow conditions. When considering the reference times of the rising limb of all BTCs, it can be seen that the pair of calculated effective flow velocities (of leading edge and peak concentration) respectively ranged between 15.8 and 9.9 m/h in BTC13, and between 294.4 and 258.5 m/h in BTC7 (Fig. 3.2) (Barberá et al., 2018).

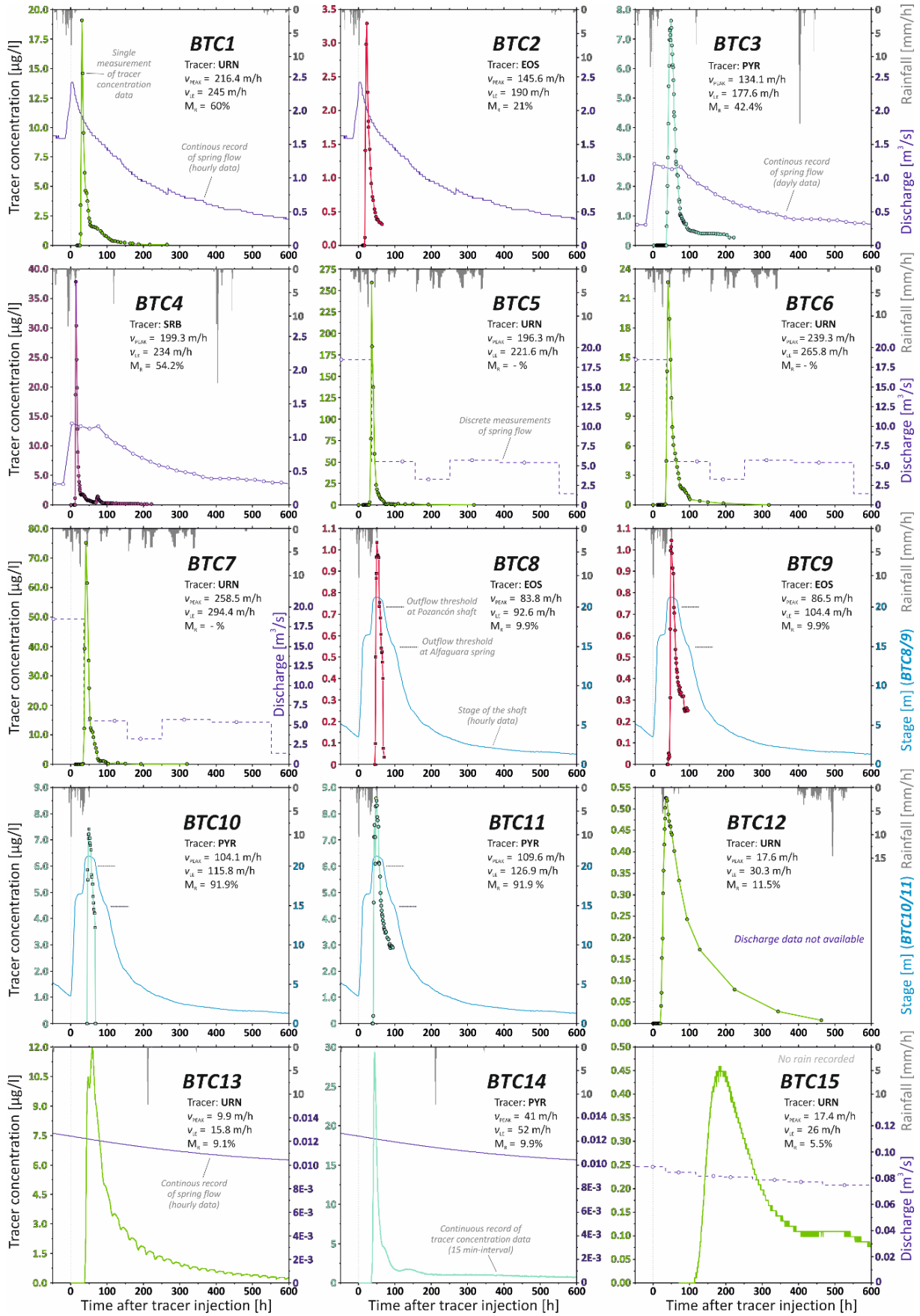


Fig. 3.2: Studied tracer break-through curves (BTCs) and spring hydrographs at sampling sites. Calculated effective velocities (V_{PEAK} and V_{LE}) and tracer recovery rates (M_R) are also shown (taken from Barberá et al., 2018).

3.3 Solute transport modeling

The BTCs were modeled by applying equilibrium and non-equilibrium transport models using the numerical code CXTFIT (Toride et al. 1995; Van Genuchten et al. 2012). The analysis of these BTCs from both graphical and numerical modeling approach allowed to characterize the solute transport at regional scale and to deeper hydrodynamic insights into several carbonate aquifers in southern Spain.

Tracer movement is mainly controlled by longitudinal advection and dispersion along the flow path length, showing an efficient longitudinal mixing under high flow conditions. Further physical processes (flow partitioning, conduit/ matrix exchange, etc.), due to tracer mass transference between the immobile and mobile conduit volume fractions would be responsible for the positive curve asymmetry and the pronounced tails observed in most of the BTCs (Fig. 3.3) (Barberá et al., 2018). The modeling of karst pathways across the thick vadose zone of the studied aquifers revealed equivalent transport modalities in both diffuse and concentrated infiltration flows which result in high velocities and effective mixing.

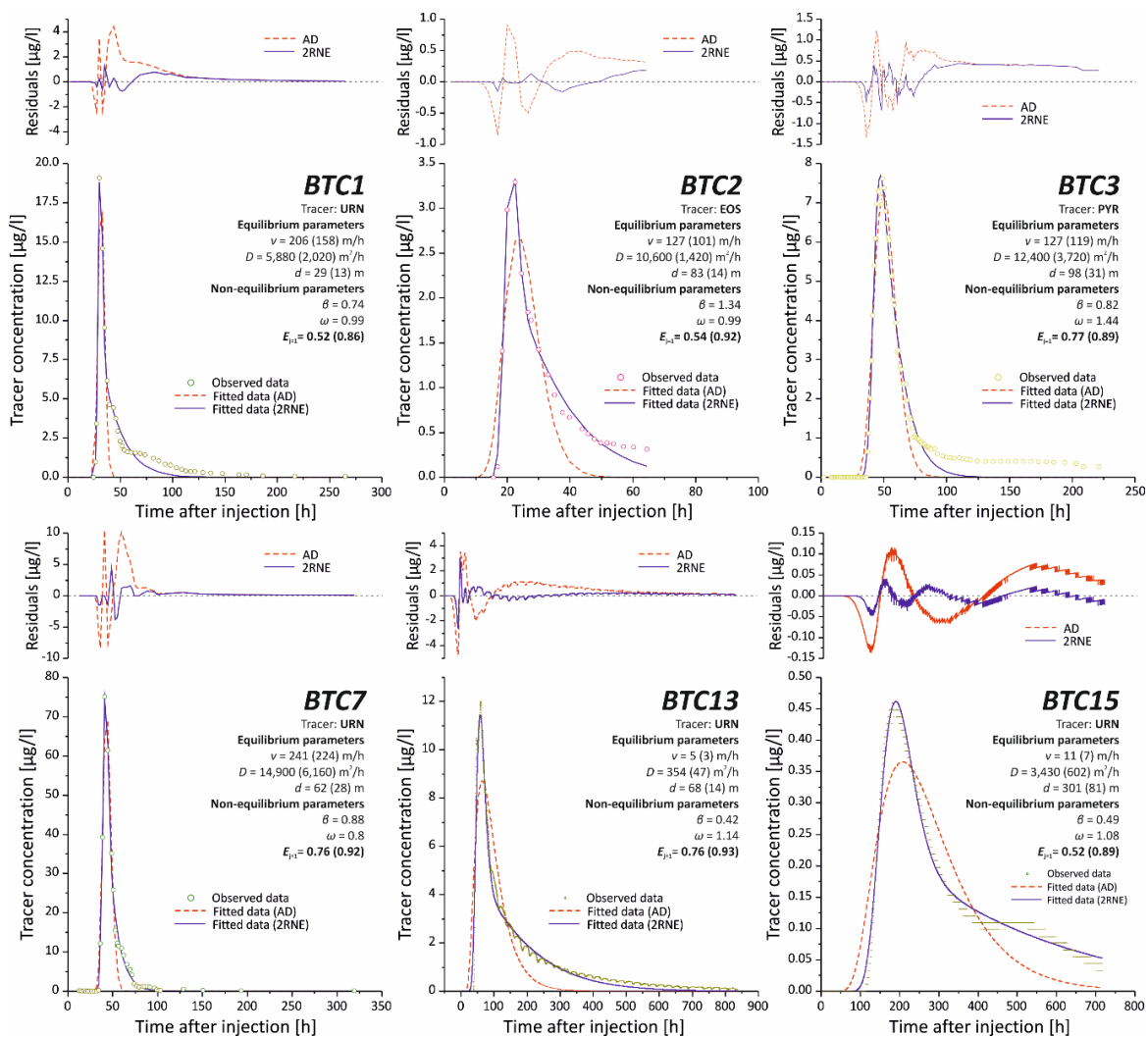


Fig. 3.3: Transport simulation results of selected BTCs (representing distinctive morphologies) based on the application of AD and 2RNE equations. The equilibrium and non-equilibrium parameters (v , D , d , β and ω) estimates, as well as the evolution of residual concentrations, are shown. Note that the values in brackets match the parameter estimation from the 2RNE transport model.

In contrast, under low flow conditions, a near steady-state situation is established within the groundwater-saturated conduit systems and the tracer migration is mainly conditioned by variable hydrodynamic interactions with the immobile conduit volume fraction. The regional evaluation of karst

underground flow properties from tracing tests consists an exceptional tool for decision makers in order to optimize groundwater management and designing protection strategies.

3.4 Planned tracer test

The aquifer systems studied in Barberá et al., 2018 are analogous to the karst aquifers that compose KARMA test sites in Spain (Eastern Ronda Mountains and Ubrique) regarding geological and hydrogeological features. In the framework of KARMA project, different tracer tests in both test sites are planned for the upcoming hydrological year and the data acquired in these previous tracer test supposes a solid base for designing future tracing experiments.

3.5 References

- Barberá JA, Mudarra M, Marín A, Andreo B, Vadillo P, Neukum C, Sánchez D, Pérez I, Ortega L (2012) Diferenciación hidrogeológica de acuíferos kársticos en la cuenca alta del río Turón (Serranía de Ronda oriental) mediante un ensayo multitrazador [Hydrogeological differentiation of carbonate aquifers in the headwaters of the Turon River basin (eastern Ronda Mountains) from a multi-tracing experiment]. *Geogaceta* 52:145–148
- Barberá JA, Andreo B (2015) Hydrogeological processes in a fluviokarstic area inferred from the analysis of natural hydrogeochemical tracers: the case study of eastern Serranía de Ronda (S Spain). *J Hydrol* 523:500–514
- Barberá JA, Andreo B (2017) River-spring connectivity and hydrogeochemical interactions in a shallow fractured rock formation: the case study of Fuensanta River Valley (S Spain). *J Hydrol* 547:253–268
- Barberá, J.A., Mudarra, M., Andreo, B. and De la Torre, B. (2018) Regional-scale analysis of karst underground flow deduced from tracing experiments: examples from carbonate aquifers in Malaga province, southern Spain. *Hydrogeol J* 26, 23–40
- De la Torre B, Mudarra M, Andreo B, Bertrand C. (2017). Hydrogeological characterization of geologically complex karst aquifer using natural responses: an example from Andalusia, southern Spain. In: Renard P, Bertrand C (eds) *Eurokarst 2016*, Neuchâtel: advances in the hydrogeology of karst and carbonate reservoirs, vol VI. Springer, Heidelberg, Germany, 285–293 pp
- Martín-Algarra A (1987) Evolución geológica alpina del contacto entre las Zonas Internas y las Externas de la Cordillera Bética [Alpine geologic evolution of the contact between Inner and Outer Zones of the Betic orogen]. PhD Thesis, University of Granada, Spain, 1171 pp
- Mudarra M (2012) Importancia relativa de la zona no saturada y zona saturada en el funcionamiento hidrogeológico de los acuíferos carbonáticos: caso de la Alta Cadena, Sierra de Enmedio y área de Los Tajos (provincia de Málaga) [Relative importance of the unsaturated and saturated zones in the hydrogeological functioning of the carbonate aquifers: the case example of the Alta Cadena, Sierra de Enmedio and Los Tajos karst areas (Málaga Province)]. PhD Thesis, University of Malaga, Spain, 557 pp
- Mudarra M, Andreo B, Marín AI, Vadillo I, Barberá JA (2014) Combined use of natural and artificial tracers to determine the hydrogeological functioning of a karst aquifer: the Villanueva del Rosario system (Andalusia, southern Spain). *Hydrogeol J* 22(5):1027–1039
- Toride N, Leij F, van Genuchten M (1995) The CXTFIT code for estimating transport parameters from laboratory or field tracer experiments, version 2.0. US Salinity Laboratory, Agricultural Research Services, USDA, Riverside, CA, 121 pp
- Van Genuchten M, Simunek J, Leij F, Toride N, Sejna M (2012) STANMOD: model, use, calibration and validation. *Am Soc Agric Biol Eng* 55(4):1353–1366

4. Lez spring catchment (France)

4.1 Field site description

The Lez system is located north of Montpellier (southern France) and consists of a major Cretaceous and Jurassic limestone karstic aquifer that supplies drinking water to about 350,000 inhabitants of the metropolitan Montpellier area (Fig. 4.1, Fig. 4.2). This large karst system located in the Mediterranean basin, South East of France, is referred to as the Lez aquifer because it feeds the Lez spring (mean discharge ca. 2200 l/s). The present water management scheme allows pumping at higher rates than the natural spring discharge during low-flow conditions, while supplying a minimum discharge rate (ca. 230 l/s) into the Lez river to ensure ecological flow downstream, and reducing flood hazards via rainfall storage in autumn (Avias 1995; Jourde et al. 2014). The Lez aquifer is located in the karst Garrigues area, which is encompassed between the Hercynian basement of the Cévennes to the north and the Mediterranean Sea to the south. The boundaries of the Lez aquifer system can be roughly materialized by the Hérault and Vidourle rivers (western and eastern sides) and by the Cévennes fault and Montpellier faults (southern and northern sides). It is ranked between the Cévennes crystalline massive at the north, and the littoral plain at the south. The topography rises gently from the south to the north of the area. The topographical heights range from 15 m.a.s.l (Vidourle's banks) to 658 m.a.s.l (Saint-Loup mountain).

The Lez spring (65 m.a.s.l), is located about 15 km north of Montpellier. It is of Vauclosian-type with a maximum discharge of approximately 15 m³/s. However, the discharge at the Lez spring is generally small or null due to the active pumping management of the aquifer, which supplies about 30 to 35 Mm³ of water per year to the metropolitan area of Montpellier and also reduces downstream floods (Jourde et al. 2014). The aquifer also discharges into several seasonal overflowing springs, the largest corresponding to the Lirou Spring (85 m.a.s.l), where high turbidity occurs during high discharge events.

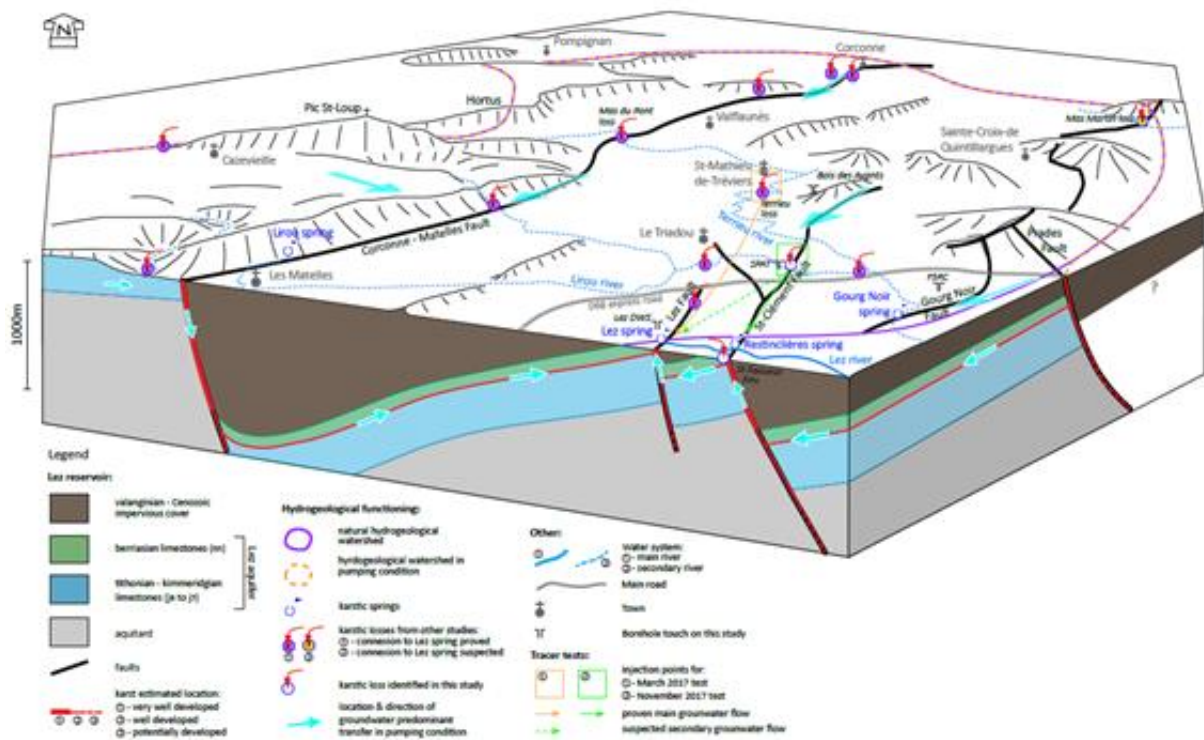


Fig. 4.1: 3D-Bloc-model of the Lez aquifer (Clauzon et al., 2020).

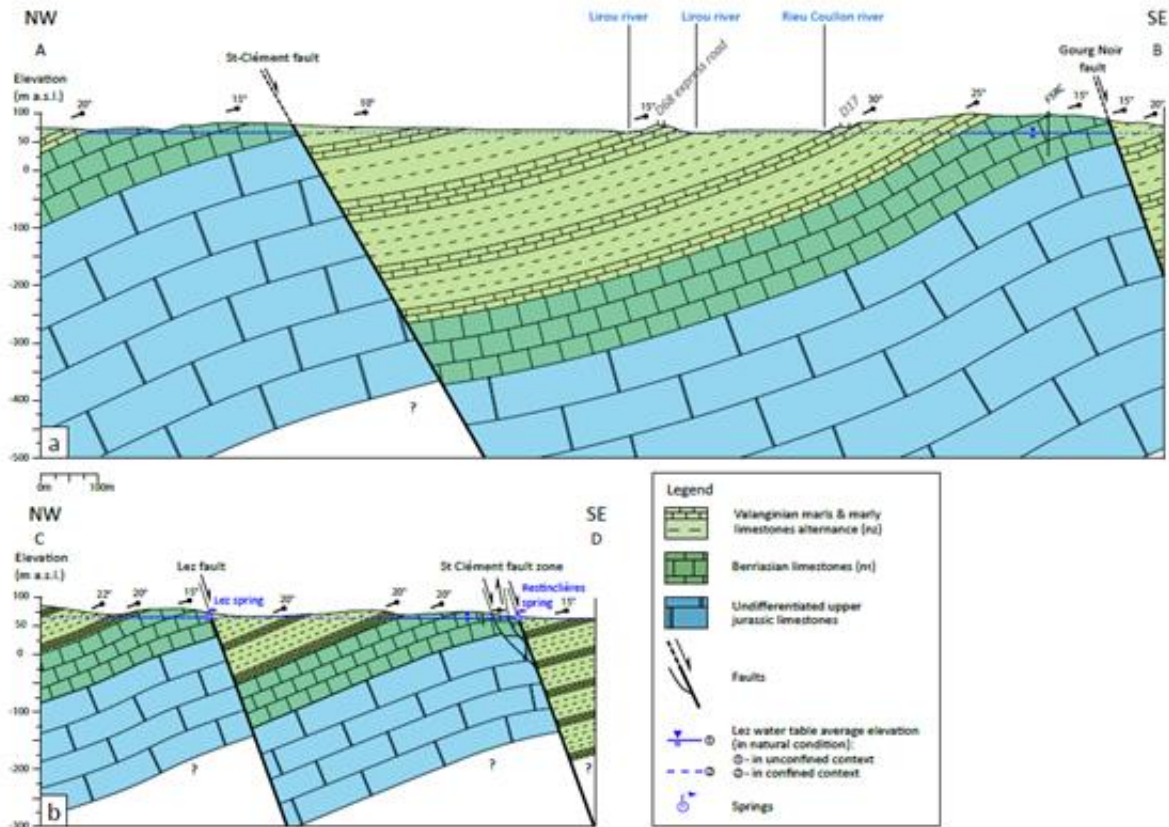


Fig. 4.2: Geological cross sections based on geological mapping and ERT investigations (Clauzon et al., 2020).

4.2 Tracer tests

Many tracer tests have been conducted in the basin since the 1960s to determine the hydraulic connections and underground water transit times. These tracer tests allowed to highlight several hydraulic continuities across the recharge area and the Lez spring and so helped in defining the Lez Spring's recharge area (Fig. 4.3).

However, the findings of most of these tests are questionable because of the detection methods used at this time (mainly active carbon and visual detection). In the framework of the 'Lez karst catchment multipurpose management' project (Jourde et al. 2011; Léonardi et al. 2012) five new tracing tests were conducted to check some uncertain tracings and outline the limits of the Lez spring groundwater basin (Fig. 4.3). One of these tracing tests, denoted GMU 1, highlighted a hydraulic continuity between Fausse Monnaie aven and the Lirou spring as well as Lez Spring. The recovery rate was around 35% and 15% at the Lirou spring and Lez spring respectively. Another tracing tests, denoted GMU 4, highlighted the hydraulic continuity from the Brestalou loss to the Lez spring with a good recovery rate above 60% for a distance of transport around 16.6 km. Such a result testifies the direct connection to the main drainage system through the Corcone fault. The other tracing tests provided negative results, although the observation period was long enough to ensure the observation of potential late recovery. More information can be found in Dausse (2015).

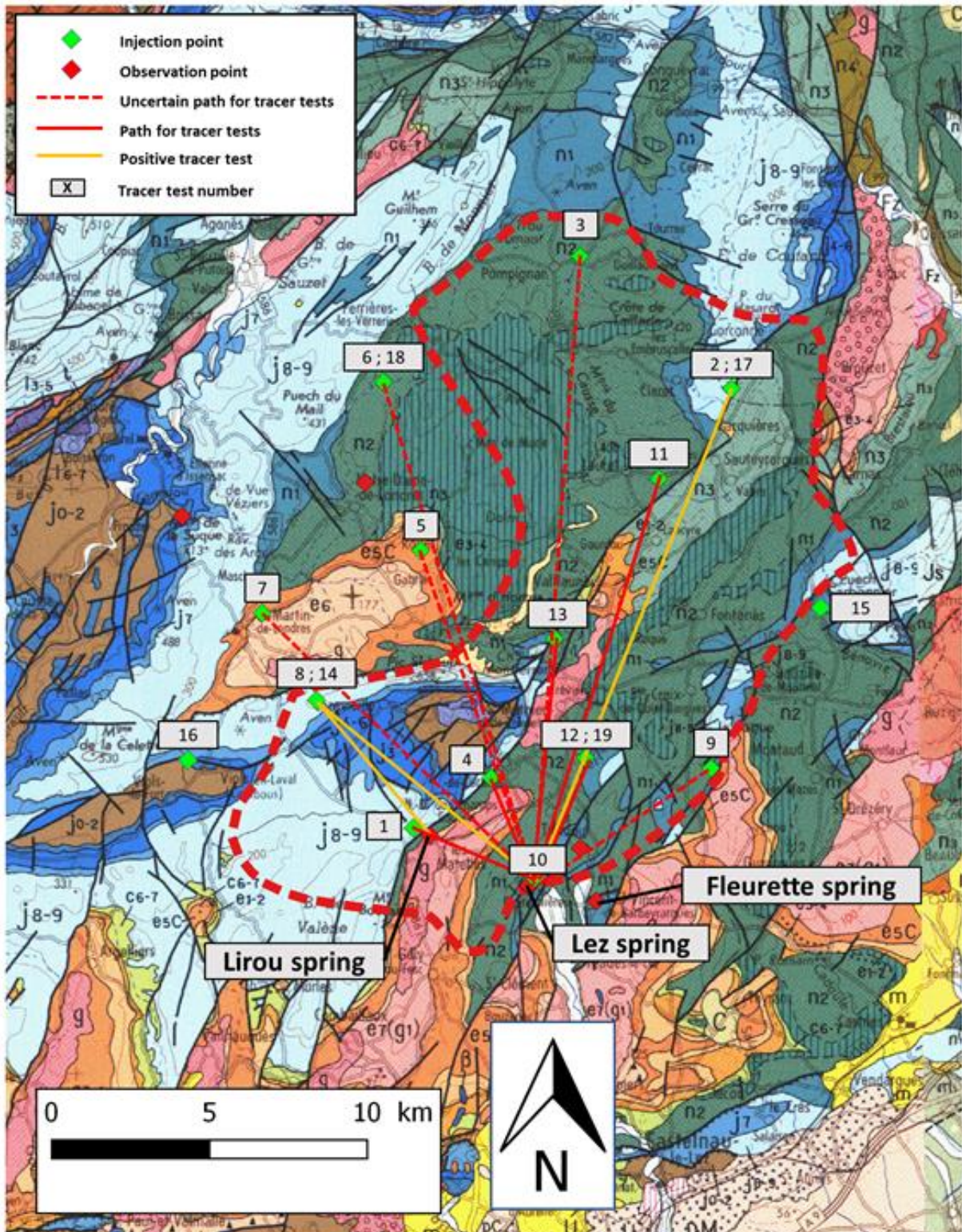


Fig. 4.3: Pattern of artificial tracer tests and boundaries of the presumed Lez spring groundwater basin under a natural flow regime (modified after Leonardi et al., 2013).

In addition, Clauzon et al. (2020) performed two tracing tests. The first tracing test was performed in March 2017 while the Lez spring outflows around $2.2 \text{ m}^3/\text{h}$. The injection took place in an active loss located in the bed of Terrieu intermittent river approximately 4.4 km following a direct N–NE line from the source of the Lez River. During the tracer test, only a positive restitution at the Lez Spring was confirmed. Many tracer tests (P. Brunet et al., CNRS, unpublished data, 2014–2018) carried out between the Terrieu River loss and Lez and Restinclières springs, have demonstrated that the

restitution at Restinclières Spring was consistently weak, uncertain or negative. This information leads to the idea that the Lez Spring drains the huge majority of the flows from the Terrieu River loss.

The second tracer test was performed in November 2017 while the Lez spring outflowed around $1.6 \text{ m}^3/\text{h}$. The injection point was the SPAT borehole located in the St-Clément fault zone following a 1.8 km direct line in the N–NE direction from the Lez Spring (Hérault). The tracer test demonstrated a strong physical connection between the SPAT borehole and Restinclières Spring with a recovery rate of around 57% and a low longitudinal dispersion coefficient ($408 \text{ m}^2/\text{h}$) which suggests that there is also a connection between the SPAT borehole and the Lez Spring.

The mean velocity observed within these two tracer tests were around 24.9 m/h and 33.3 m/h respectively. The same order of magnitude has been observed with the maximal velocity estimated considering the linear distance between injection and recovery points, including the historic tracing tests, with mean velocity around 33 m/h (calculated based on 21 tracing tests where the required information is available).

Since the historic tracing tests do not provide a complete BTC, only the recent tracing tests have been interpreted with a physical based model. Dausse (2015) estimates a longitudinal dispersion coefficient ranging from 1152 to $8784 \text{ m}^2/\text{h}$ at the regional scale with a dual region dispersion equation model. At the local scale (Terrieu experimental site) the longitudinal dispersion coefficient ranges from 0.54 to $2.01 \text{ m}^2/\text{h}$. In addition, Clauzon et al. (2020) estimates a longitudinal dispersion coefficient of 540 and $408 \text{ m}^2/\text{h}$.

Among all the tracing tests performed within the Lez system both unimodal and bimodal BTC have been observed. The tracing test from the Brestalou loss presents the highest transport speeds and a restitution composed of a single peak in concentration. This can be explained by a flow concentrated in the main drainage zone parallel to the Corconne fault, directly connected to the Lez source. Conversely, multimodal BTC has been observed on both regional scale and local scale (Terrieu experimental site). At the regional level, during the tracing test from the Fausse Monnaie aven, the restitution measured at the Lez source shows two concentration peaks. The fact that there are no successive rainfall events and that the flow of the Lez source is in recession during the restitution of these two peaks, suggests the existence of two separate drainage systems from the Fausse Monnaie aven to the source of the Lez. Several hypotheses concerning the organization of the drainage system are possible: (1) existence of two flow paths shortly after the injection zone, with a path to the Lirou spring and another going directly to the Lez spring; (2) a single flow path along a main drainage axis towards the Lirou spring (major direction of karstification of the Causse de Viols-le-Fort) which would then separate into two flow paths near the Corconne fault.

The whole tracer tests database allowed to determine a certain range of variability in transport velocities depending on the hydrology conditions during tracer test, and heterogeneity in flow processes concerning the various tracing systems. Fig. 4.4 gives information about hydrological condition for each tracer tests based on (1) the measured rainfall during the 7 and 14 days before tracer injection and (2) the observed discharge during tracer tests compared with mean and interquartile discharge at Lez's spring, as an integrative variable of the flow condition across the catchment. In addition, Fig. 4.5 gives a quick overview of the observed transport velocities across the Lez's catchment.

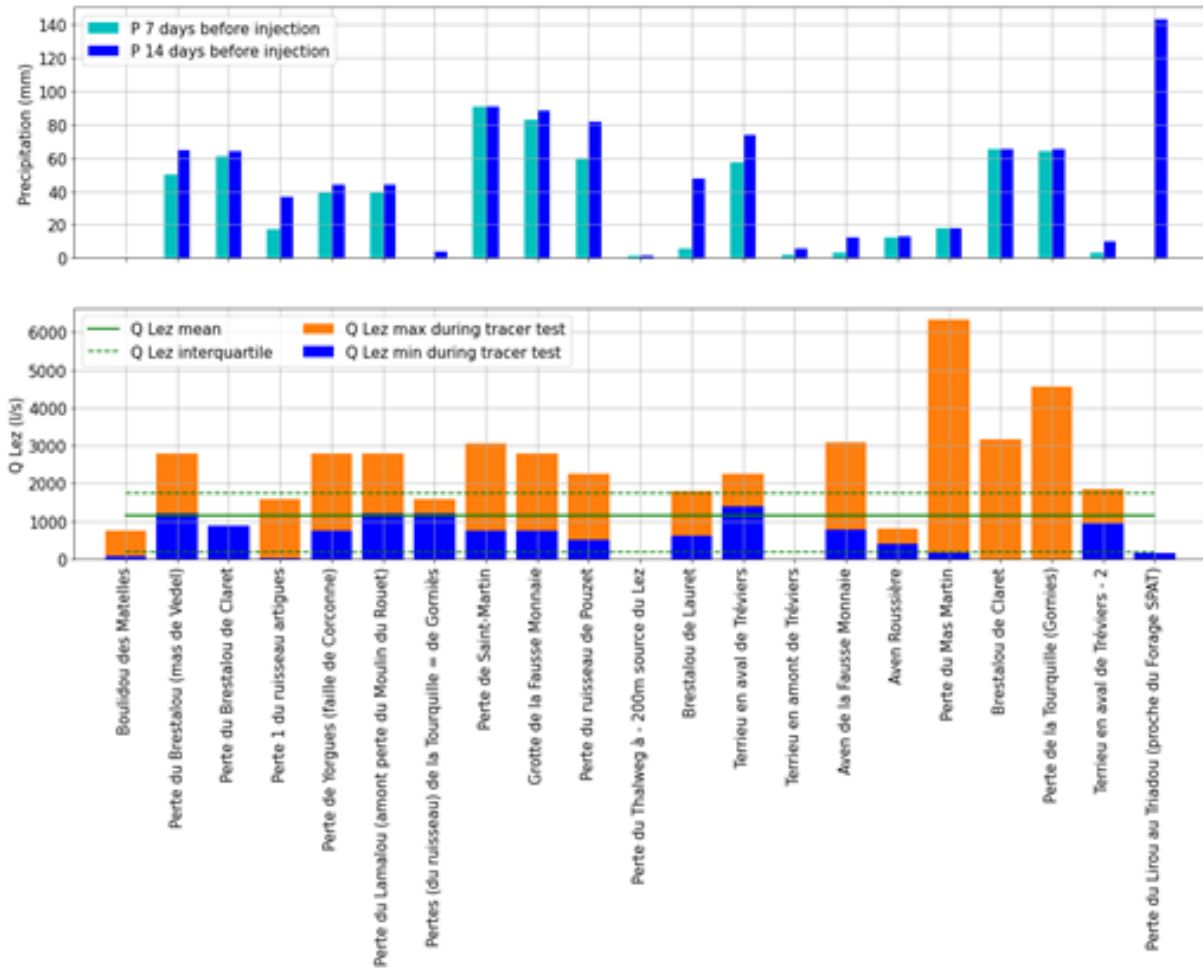


Fig. 4.4: Overview of the hydrological conditions during the tracer tests.

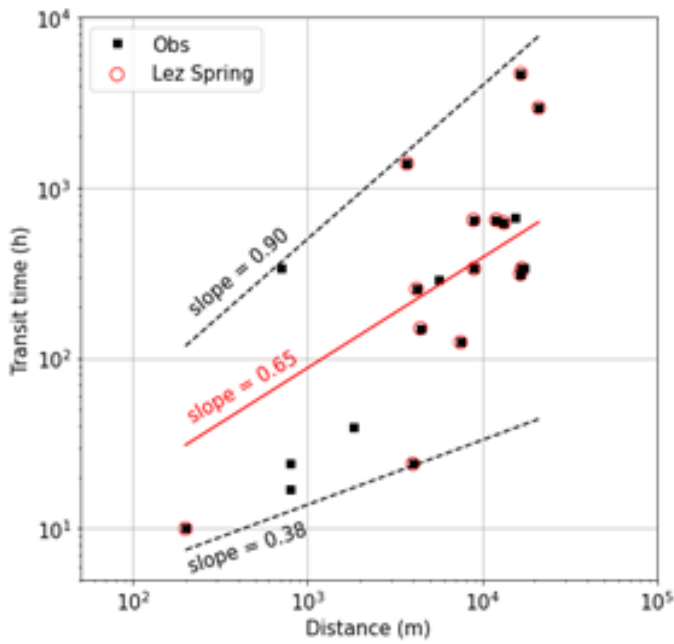


Fig. 4.5: Log-log representation of the apparent transport velocities. Tracer tests with recovery observed on the Lez spring are presented in red.

4.3 References

Avias JV (1995) Gestion active de l'exurgence karstique de la Source du Lez (Hérault, France) 1957-1994. *Hydrogéologie (Orléans)* 113–127

Clauzon V, Mayolle S, Leonardi V, et al (2020) Fault zones in limestones: impact on karstogenesis and groundwater flow (Lez aquifer, southern France). *Hydrogeol J.* <https://doi.org/10.1007/s10040-020-02189-9>

Dausse A (2015) Facteurs d'échelle dans la hiérarchisation des écoulements au sein d'un aquifère karstique. Thèse de Doctorat, Université de Montpellier

Jourde H, Dörfliger N, Maréchal J-C, et al (2011) Projet gestion multi-usages de l'hydrosystème karstique du Lez - Synthèse des connaissances récentes et passées. BRGM

Jourde H, Lafare A, Mazzilli N, et al (2014) Flash flood mitigation as a positive consequence of anthropogenic forcing on the groundwater resource in a karst catchment. *Environ Earth Sci* 71:573–583. <https://doi.org/10.1007/s12665-013-2678-3>

Leonardi V, Jourde H, Dausse A, et al (2013) Apport de nouveaux traçages et forages à la connaissance hydrogéologique de l'aquifère karstique du Lez. *Karstologia* 7–14

Léonardi V, Jourde H, Maréchal J-C (2012) Projet gestion multi-usages de l'hydrosystème karstique du Lez - Résultats complémentaires des forages et traçages. BRGM

5. Gran Sasso (Italy)

5.1 Field site description

The Gran Sasso hydrostructure is defined as a calcareous-karstic aquifer system of about 1034.4 km² of total extension and it is the most representative karst aquifer of the central-southern Apennines. The interest in this area is linked to the huge amount of groundwater resources usable for human purposes, to the enhancement and protection of protected areas (Monjoie, 1980) but also to both anthropogenic problems, such as the construction of the Gran Sasso motorway tunnel. The strategic role of the karst system is defined by the high quality of the water, guaranteed also by a limited anthropization of the territories in which they generally develop, and by the water quantities that these systems are able to host.

The Gran Sasso hydrogeological system is characterised by Meso-Cenozoic carbonate units (aquifer), bounded by terrigenous units represented by Miocene flysch (regional aquiclude) along its northern side, and by Quaternary continental deposits (regional aquitard), along its southern side (Petitta and Tallini, 2002).

The fracturing and the karstification of the Gran Sasso calcareous complex is influenced mainly by the stratigraphy and the structural elements, which often act as an obstacle to the groundwater flow causing the presence of different groundwater watersheds and influencing the direction of the flow paths. The preferential directions of groundwater flow are locally conditioned by the main tectonic discontinuities and are guided by the heights of the hydrogeological limits. In fact, most of the groundwater is directed towards the most depressed sectors of the aquifer, where the limits of permeability are placed at lower altitudes, moving through a regional groundwater flow. This movement within the aquifer is due to the local presence of karst features that promote infiltration. Furthermore, the karst conduit system of the Gran Sasso aquifer is uniform and well interconnected. The underground karst system is not very widespread, and the cavities generally reach modest dimensions, feeding only some of the main springs of the hydrogeological basin. There are numerous small-scale karst forms such as sinkholes and fields. A complete description of the aquifer characteristics is available in D2.1 (Preliminary Water Budget).

The Gran Sasso aquifer feeds spring groups, located at different altitudes along the low permeability boundary, with a huge discharge of more than 18 m³/s (Adinolfi Falcone et al., 2008). These springs have been organized into six groups based on groundwater flow and hydrochemical characteristics, as illustrated in Figure 1 (Barbieri et al., 2005). The springs of group A are fed on the northern boundary, lying near the no-flow limit due to the main thrust.

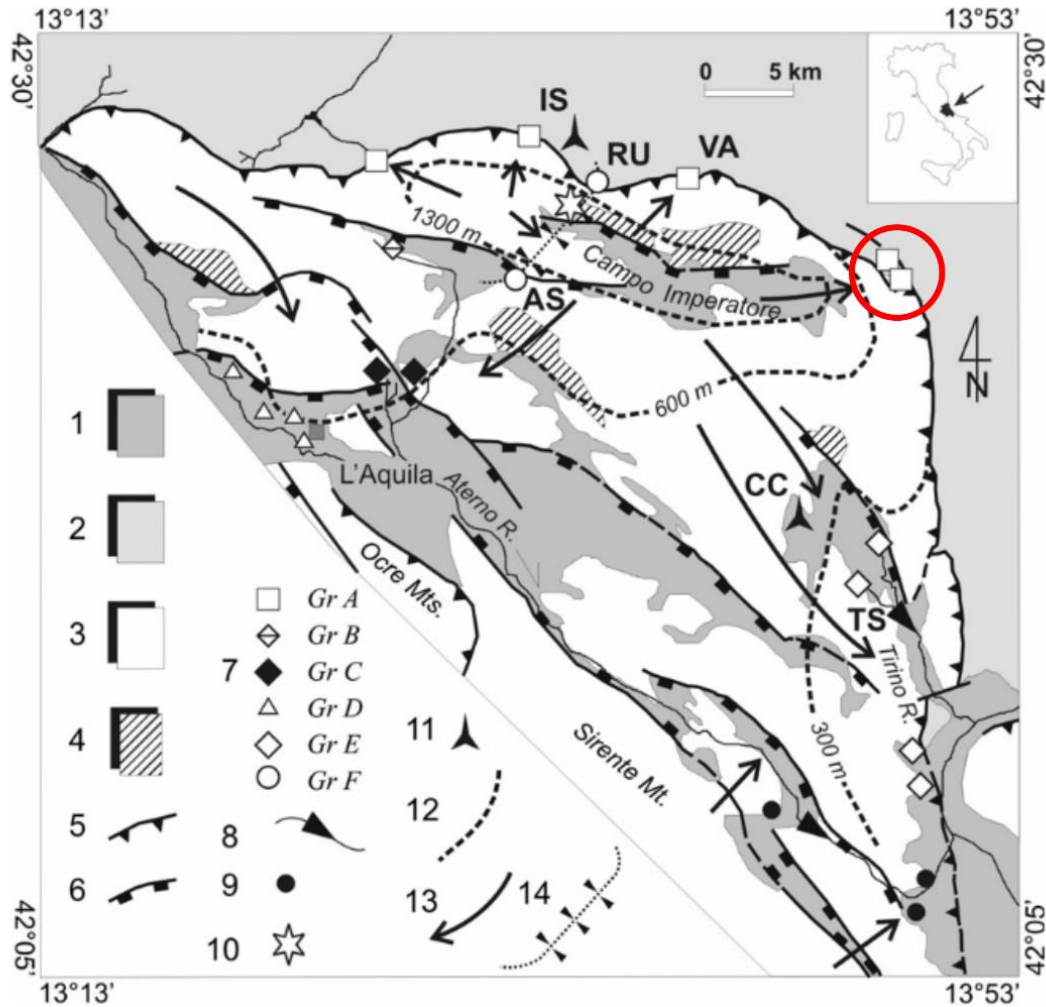


Fig. 5.1: Gran Sasso hydrogeological outline. The red circle shows the two studied springs for the tracer tests. 1: aquitard (continental detrital units of intramontane basins, Quaternary); 2: aquiclude (terrigenous turbidites, Mio-Pliocene); 3: aquifer (calcareous sequences of platform Meso-Cenozoic); 4: low permeability substratum (dolomite, upper Triassic); 5: thrust; 6: extensional fault; 7: main spring: AS: Assergi drainage; RU: Ruzzo drainage; VA: Vacelliera spring; TS: Tirino springs; symbols refer to the six spring groups identified in Barbieri et al. (2005); 8: linear spring; 9: springs belonging to a nearby aquifer; 10: INFN underground laboratories (UL in the text); 11: meteorological station (IS: Isola Gran Sasso, CC: Carapelle Calvisio); 12: presumed water table in m asl; 13: main groundwater flow path; 14: highway tunnels drainage. [Amoruso, 2012]

Among the springs of group A, Mortaio d'Angri and Vitella d'Oro springs (red circle in Fig. 5.1) are located on the north-eastern side of the aquifer. These springs have a limited discharge, between $0.28 \text{ m}^3/\text{s}$ and $0.38 \text{ m}^3/\text{s}$. Both springs, tapped for drinking purposes, are fed by a minor hydrogeological basin, but their main characteristics are the interconnection between the Mortaio d'Angri spring, directly fed by the carbonate aquifer of Gran Sasso, and the Vitella d'Oro spring, fed by conglomerate deposits derived by paleo-landslides on the NE slope of the massif, as resumed in Fig. 5.2. In these conglomerates (Rigopiano Conglomerates) a karst network progressively evolved, and this development reflects in an impulsive regime of the Vitella d'Oro spring, which is tapped by an underground drainage tunnel. Fig. 5.2 resumes the details of the karst flowpaths between the recharge area, where some small swallow holes have been identified. Also a clear decrease has been observed in the Rigopiano stream discharge until the complete disappearance of surface flow downstream.

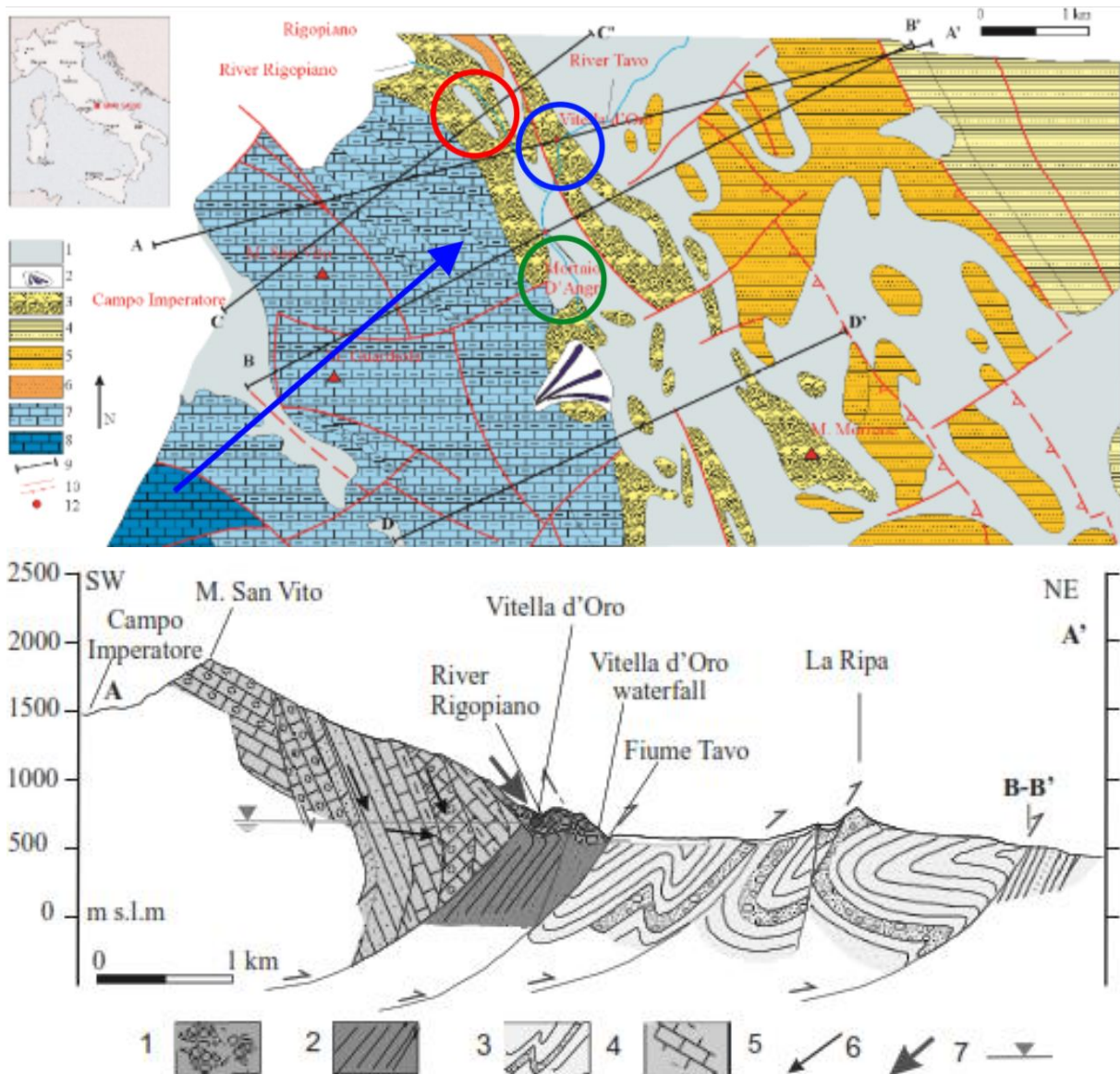


Fig. 5.2: Vitella d'Oro hydrogeological outline. Above: the red circle identifies the recharge area, the blue one the Vitella d'Oro spring and the green one the upgradient Mortaio d'Angri spring. Blue arrow represents the regional groundwater flow direction. Below: hydrogeological section from Ferracuti et al, 2006 (modified).

Recorded discharge at Vitella d'Oro spring, both tapped and overflow contributions, are resumed in Fig. 5.3. It is evident that historical mean discharge of about 380 L/s does not include the variable overflow. The spring is characterized by high turbidity events after heavy rainfall events and in general during Spring (snowmelt period) and Autumn (high rainfall rate) (Rusi et al. 2016).

For such peculiar hydrogeological conditions, a tracer test has been scheduled and organized for Spring 2021, but the Covid-19 pandemic pushes to postpone the tracer test, which is now scheduled for Summer 2021.

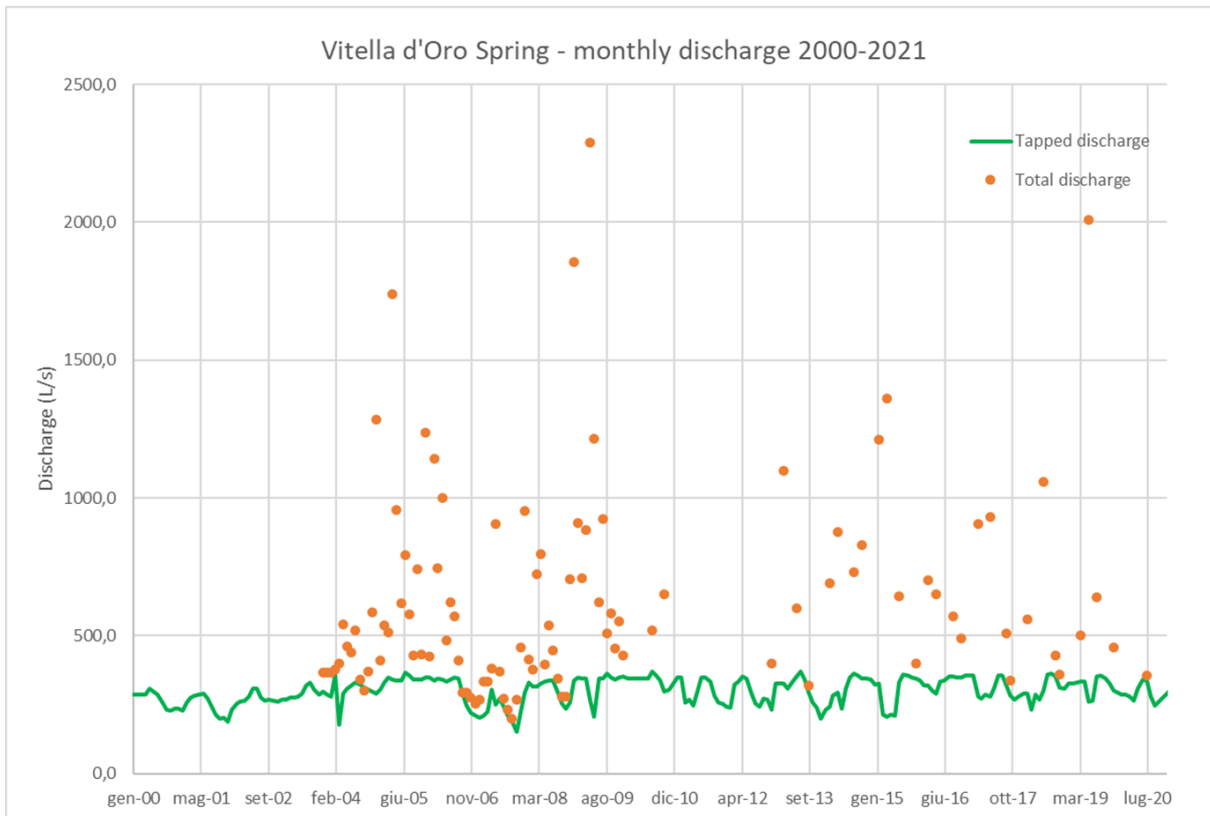


Fig. 5.3: Vitella d'Oro discharge during last twenty years. The tapped values are in green and the measured total overflow is represented by the orange dots.

5.2 Planned tracer tests

The planned tracer test intends to use two tracers, Uranine and Sodium-Naphthionate, considering the previous experiences and the related useful suggestions provided by the KIT team during preliminary discussions. KIT team is invited to participate in the field test, but due to the Covid-19 pandemic, URO will directly coordinate the field activities. KIT will help with tracer analysis and related result interpretations. The selected tracers are of common use in karst hydrogeology and their impact and toxicity on ecosystems is null (Behrens et al, 2001).

Uranine is the sodium salt of fluorescein and has a high solubility in water and a very low detection limit for fluorimeter, both in field and in laboratory (Hess, 2008; Goldscheider et al., 2008). Sodium-Naphthionate is invisible, has a low detection limit, but can interfere with DOC; considering that no significant concentrations of DOC have been recorded at Vitella d'Oro spring in the past, this tracer seems to be useful for the planned test. The test is scheduled for July 2021, but depending on the flow conditions of the spring it could be postponed until September 2021, because of the low flow conditions observed in June 2021. We are currently waiting for the final approval by the Local Authorities.

The test procedure has been set up together with the KIT team, which gently provided the tracer amount necessary for the activity. Before field injection, the tracers will be diluted in 1-2 litres of water. Injection points will be one or both existing swallow holes (Fig. 5.4) and/or in the streambed where surface water clearly infiltrates in the subsoil.

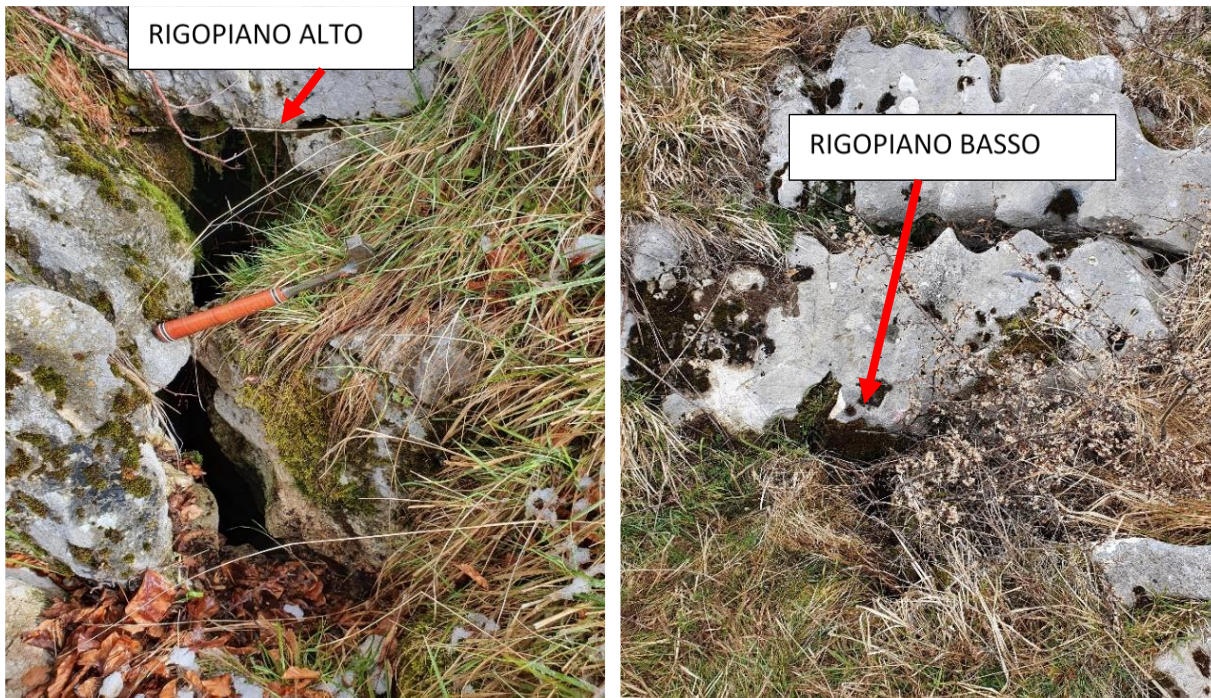


Fig. 5.4: Swallow holes in the recharge area of Vitella d'Oro spring, selected for the tracer test.

To correctly estimate the tracer mass to be used for the test, simplified advection/dispersion 1D models have been run, and related results have been compared by the observed turbidity events (Ferracuti et al., 2006). Time interval ranging from 3 to 6 hours is expected for tracer arrival at the spring tapping system, where an Albillia FL30 Fluorimeter (Schneegg, 2002) will record the tracer concentration with time (acquisition frequency: 5-10 minutes), giving the possibility to separate the signals of each tracer (Schneegg et al., 2012). A second Fluorimeter FL30 will be placed downstream along the Tavo River, to check possible arrival independently from the tapped spring. Simulation results allow to evaluate the initial mass to be used in the injection point, which has been established in 20 g of Uranine and 100 g of Sodium-Naphthionate. Additional points for tracer arrival will be monitored by charcoal bags, including the Mortaio d'Angri spring, its related pumping wells and the surface streams existing in the area.

5.3 References

Barbieri M., Boschetti T., Petitta M., Tallini M. (2005) Stable isotopes (2H , 18O and $87/86\text{Sr}$) and hydrochemistry monitoring for groundwater hydrodynamics analysis in a karst aquifer (Gran Sasso, Central Italy). *Applied Geochemistry*, 20 (11), 2063-2081, IF=2.261

Adinolfi Falcone R., Falgiani A., Parisse B., Petitta M., Spizzico M., Tallini M. (2008) Chemical and isotopic ($18\text{O}\%$, $2\text{H}\%$, $13\text{C}\%$, 222Rn) multi-tracing for groundwater conceptual model of carbonate aquifer (Gran Sasso INFN underground laboratory – central Italy). *Journal of Hydrology*, 357,

Behrens, H., Beims, U., Dieter, H., Dietze, G., Eikmann, T., Grummt, T., Hanisch, H., Henseling, H., Käß, W., Kerndorff, H., Leibundgut, C., Müller-Wegener, U., Rönnefahrt, I., Scharenberg, B., Schleyer, R., Schloz W., Tilkes, F. (2001). Toxicological and ecotoxicological assessment of water tracers. *Hydrogeology Journal* 9, 321–325.

Ferracuti, L., Marinelli, G., & Rusi, S. (2006). Idrogeologia e monitoraggio delle sorgenti carsiche del Tavo (massiccio carbonatico del Gran Sasso) e loro implicazioni nella gestione dell'emergenza torbidità. *Giornale Di Geologia*, 3, 47–52.

- Goldscheider, N., Meiman, J., Pronk, M., & Smart, C. (2008). Tracer tests in karst hydrogeology and speleology. *International Journal of Speleology*, 37(1), 27-40.
- Hess, J. W. (2008). Methods in Karst Hydrogeology. *Groundwater*, Vol. 46, pp. 172–172.
- Monjoie, A. (1980). Pr vision et contr le des caract ristiques hydrog ologiques dans les tunnels du Gran Sasso (Appenin, Italie). *Livre Jubilaire*, L. Calembert, Ed. Thone, Li ge.
- Petitta, M., & Tallini, M. (2002). Idrodinamica sotterranea del massiccio del Gran Sasso (Abruzzo): Nuove indagini idrologiche, idrogeologiche e idrochimiche (1994-2001). *Bollettino Della Societ  Geologica Italiana*, 121(3), 343–363.
- Rusi, S., Marinelli, G., Palmucci, W. (2016). La gestione dell'emergenza torbidit  delle sorgenti carsiche del Tavo (Appennino Centrale). *Atti del Convegno Nazionale "La ricerca carsologica in Italia"*, 22-23 giugno 2013, Laboratorio carsologico sotterraneo di Bossea, Frabosa Soprana, pp.155-159.
- Schnegg, P. A. (2002). An inexpensive field fluorometer for hydrogeological tracer tests with three tracers and turbidity measurement. *Articles of the Geomagnetism Group at the University of Neuch tel, Groundwater and Human Development*, pp. 1484-1488.
- Schnegg, P. A. and Thueler, L. (2012). Application of a multi-LED field fluorometer for simultaneous detection of hard to separate dye tracers and fluocapteurs. *11th Conference of Latin American hydrogeology*. 20-24 August 2012. Cartagena de Indias, Colombia.

6. Hochifen-Gottesacker (Austria)

6.1 Field site description

The test site Hochifen-Gottesacker is located at the border between Austria (Vorarlberg) and Germany (Bavaria, Fig. 6.1a) in the Northern Calcareous Alps. The total size of the catchment area of Aubach- and Sägebach Spring (Fig. 6.1b) is about 35 km² (Chen & Goldscheider, 2014). The altitude varies between 1035 m asl (Sägebach Spring) and 2230 m asl (summit of Mt. Hochifen).

The study site belongs to the Helvetic zone, which plunges underneath the Flysch nappes consisting of marl and sandstone formations on three sides (Wyssling, 1986). The most important rock formation is the Cretaceous Schratenkalk limestone layer, which forms a relatively thin karst aquifer (about 100 m) above a thick marl formation (about 250 m) acting as a regional aquitard. Previous research (Goldscheider, 2005; Goepfert and Goldscheider, 2008) have shown that the orientation of the underground flow paths is structurally controlled, i.e. the underground flow is parallel to the strata. The elevated Gottesacker terrain is a bare karren field, dominated by kluftkarren. In the lower parts, the limestones are covered with shallow rendzina soil, that is partially overgrown with coniferous forest. However, large karst outcrops without overlying soil are frequent (Goldscheider, 2002).

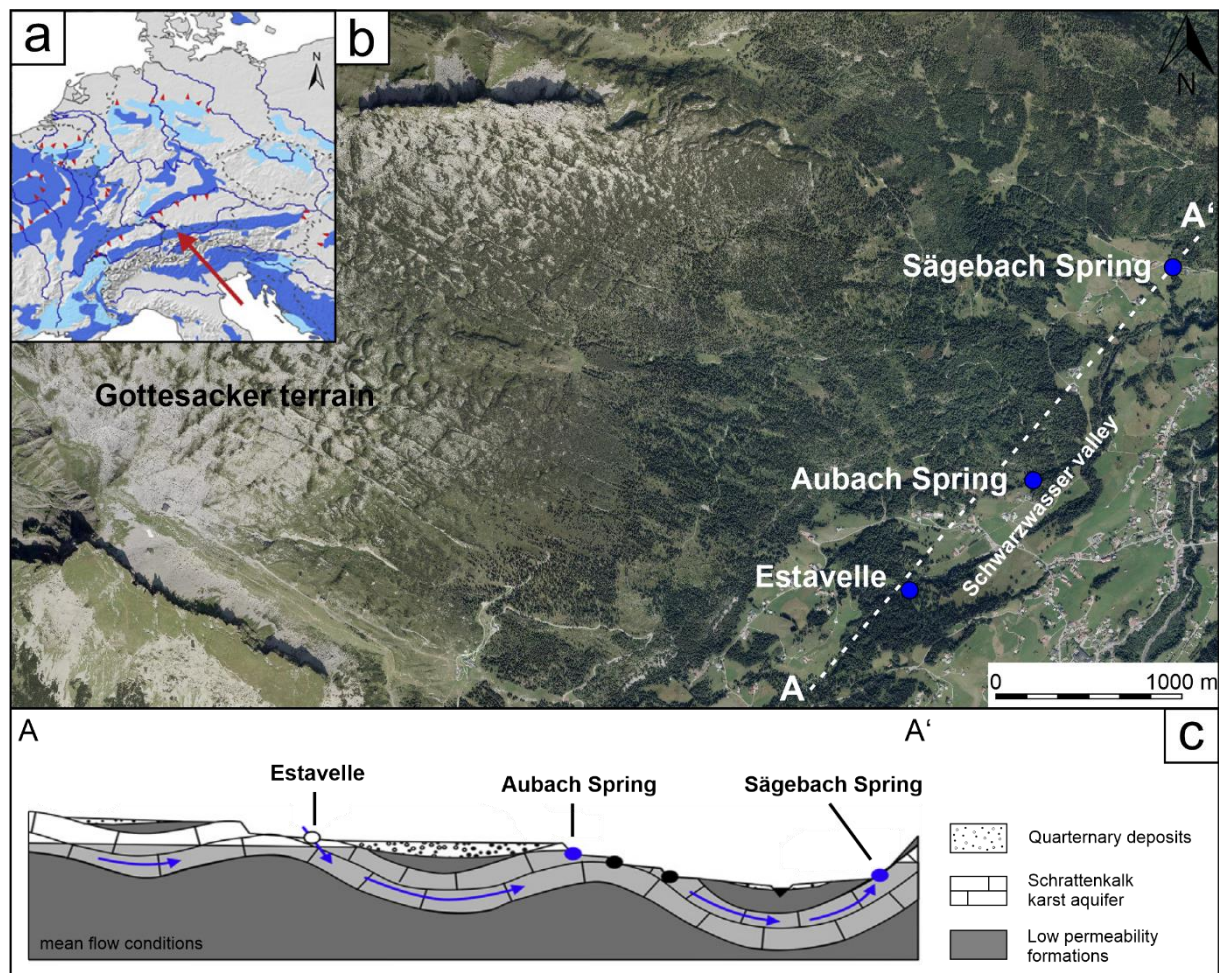


Fig. 6.1: a) Location of the test site shown on a section of the World Karst Aquifer Map (Chen et al., 2017) with carbonate rocks in blue. b) Detail of the test site with the Gottesacker area, Aubach- and Sägebach Spring and Estavelle (basemap: Land Vorarlberg – data.vorarlberg.gv.at) and c) schematic cross-section with flow paths at mean flow conditions (modified after Goepfert et al., 2020).

The mountain range SE of the Schwarzwasser valley is formed by sedimentary rocks of the Flysch zone and is mainly characterized by low permeability and drained by surface runoff. The karst aquifer in the catchment of the springs is recharged directly from precipitation, either diffuse as well as concentrated and also from surface streams that drain the part of the catchment area that consists of low permeable Flysch rocks (Chen & Goldscheider, 2014).

The climate of the study site is cool-temperate and humid. The annual average Temperature at the nearest weather station is 5.7° C while mean monthly temperatures range from 2.2° C to 14.4° C. The mean value of the annual precipitation is 1836 mm, with two maxima in June-August and December-January. Snowfall and snow accumulation usually occur between November and May (Chen et al., 2018).

The main springs in the system are Aubach and Sägebach Springs (Fig. 6.2, Fig. 6.3). The large but intermediate Aubach Spring discharges up to about 8 m³/s but runs dry in long dry periods and in winter. Further downstream, the Sägebach Spring presents the largest permanent spring in the valley and discharges up to about 3.5 m³/s (Chen & Goldscheider, 2014). Both are high alpine karst springs and currently not used for drinking water supply, therefore the water is not treated in any way. The base-flow spring (Sägebach Spring) is partly used for a hydropower plant. Both springs show a high variability regarding the water quality. After rain events, high contaminations with fecal bacteria, caused by livestock farming and wild live, can be observed.



Fig. 6.2: Photo of Aubach, 25 m downstream of the spring (Photo: Simon Frank).



Fig. 6.3: Photo of Sägebach spring (Photo: Nikolai Fahrmeier).

One special feature in the Schwarzwasser valley is the large Estavelle (Fig. 6.4), which, during low flow, acts as a swallow hole with sinking rates up to 500 L/s. During high flow conditions the Estavelle is a large karst spring (Fig. 6.5) with discharge up to 4000 L/s. Since the karst system reacts very fast, it is possible that the Estavelle turns from swallow hole to spring within a few hours.

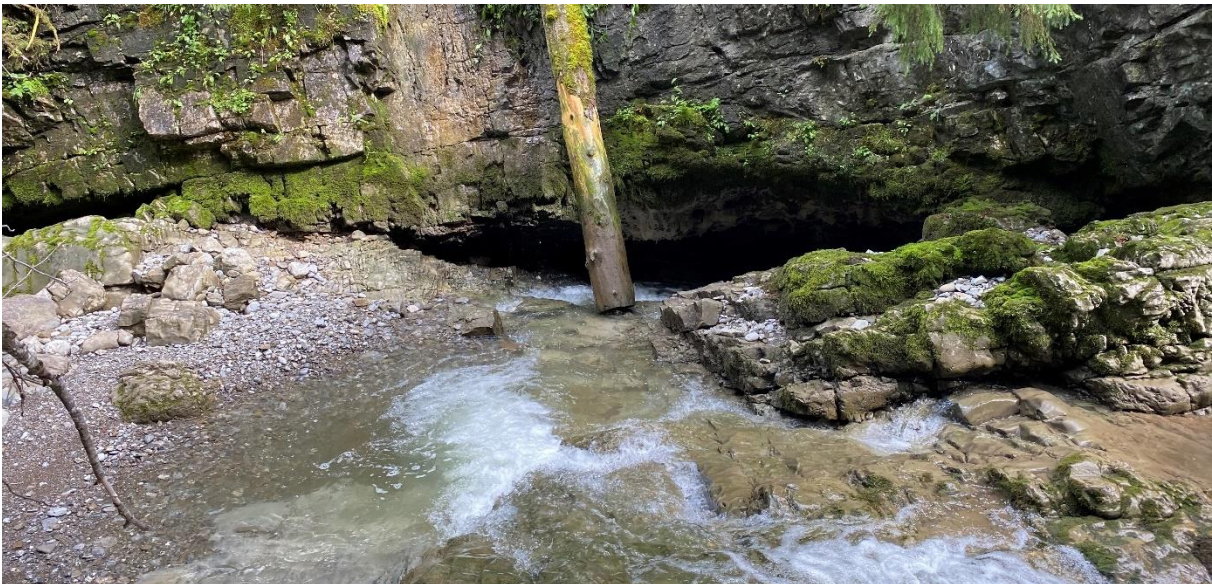


Fig. 6.4: Photo of the Estavelle, acting as a swallow hole during low flow conditions in August 2020 (Photo: Simon Frank).



Fig. 6.5: Photo of the Estavelle during high flow conditions, when the Estavelle acted as a spring in June 2021 (Photo: Nikolai Fahrmeier).

6.2 Previous tracer tests

The earliest tracer tests in the Hochifen-Gottesacker karst area were carried out between the 1940s and 1960s. These tracer tests proved the hydraulic connection between the Hölloch cave in the Mahdtal valley and the Sägebach Spring (while the tracer did not reach Aubach Spring). And other local hydraulic connections in several karst caves (Goldscheider, 2002; Wagner, 1950).

Additional tracer tests were performed in 1996, 1997 (Fig. 6.6) and 2005, 2006. In 1996 two tests were carried out in the eastern Gottesacker area and in the Schwarzwasser valley (IP2 and IP3, Fig. 6.6) where uranine and Eosine were used as tracers. In August 1997 three tracer tests were performed in the Schwarzwasser valley (IP4 – IP6, Fig. 6.6) during medium to low water conditions where uranine, Eosine and Sulforhodamin B were used as tracers and a large multi tracer test (IP7 – IP16, Fig. 6.6) was performed in September 1997 in the entire area including the Subersach and Schwarzwasser valleys where Uranine, Eosine, Sulforhodamin B, Pyranin and Sodium - Naphthionate were used as tracers.

The purpose of these tracer tests was the determination of the underground flow paths and the delineation of the catchment areas of the main springs as well as the more precise delineation of the European watershed. The tracer tests also delivered information about the hydraulic properties of the aquifer and information about the mechanisms of contaminant transport.

Altogether 1320 water samples were taken and analyzed during these tracer tests and 94 charcoal bags were also taken and analyzed in the laboratory.

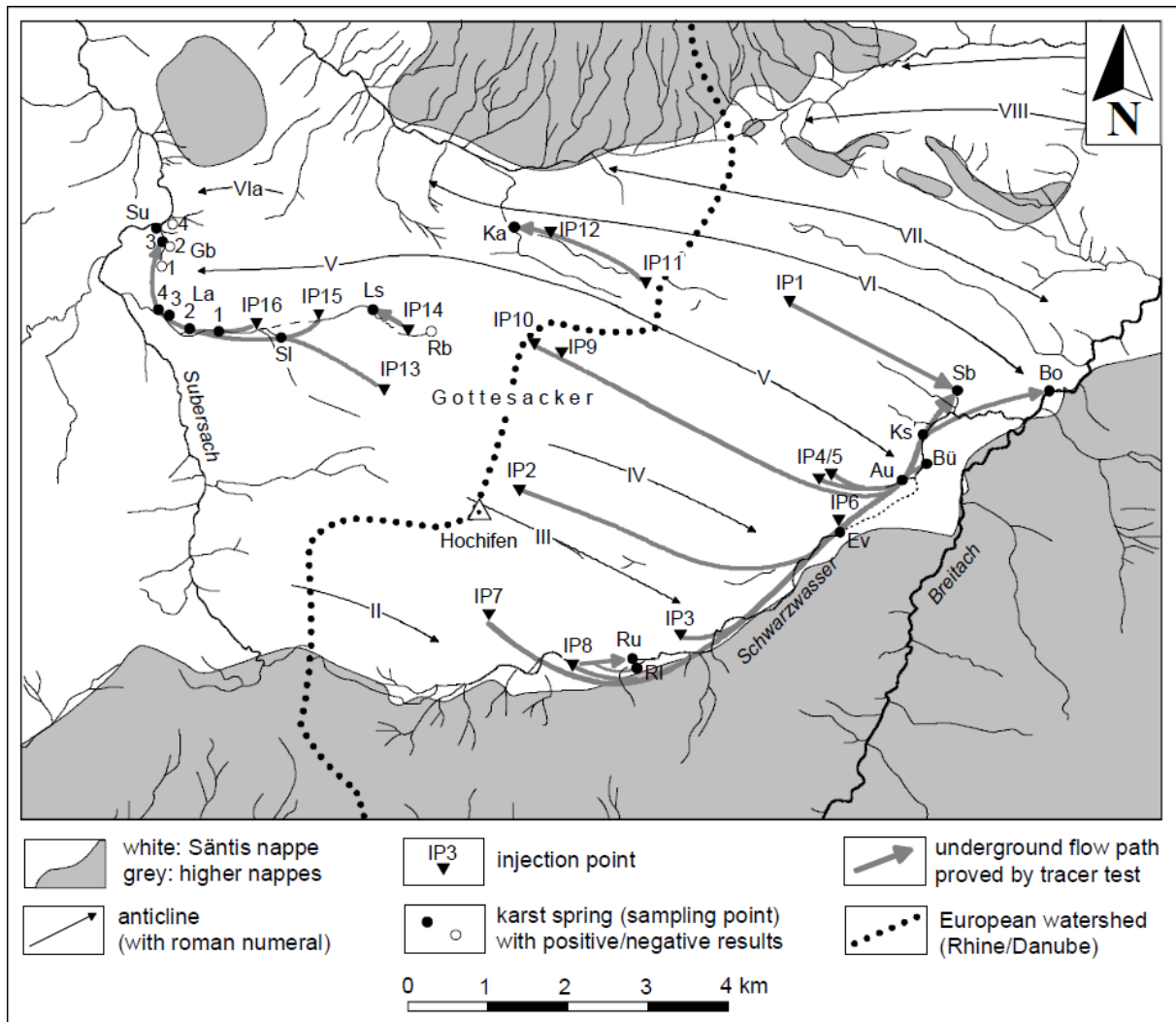


Fig. 6.6: Tracer tests in the Hochifen-Gottesacker area. Location of the injection points (IP1 – IP16), the sampling points and the proven flow paths (from Goldscheider, 2002).

In order to get a complete understanding of the underground flow paths in the entire karst system, at least one injection point was selected in each syncline both east and west of the culmination line. The injections in the central Gottesacker area were selected to more precisely locate the European watershed. The injections in the Schwarzwasser valley were carried out in order to check the function of the karst aquifer in the valley as a hydraulic connector between the karst water and the surface water of the eastern part of the area (Goldscheider, 2002). One tracer was injected in the sewage shaft of a ski station (IP2) in order to determine the influence of waste water on the springs in the valley and two injections (IP4 and IP5) were performed to check which of the springs are potentially affected by sewage water from a cave that was filled with waste before 1975 (Goldscheider, 1998).

A selection of the resulting breakthrough curves of the tracer tests are given in Fig. 6.7 and in the following section, the most important results of the tracer tests in the eastern part of the Hochifen-Gottesacker area are described.

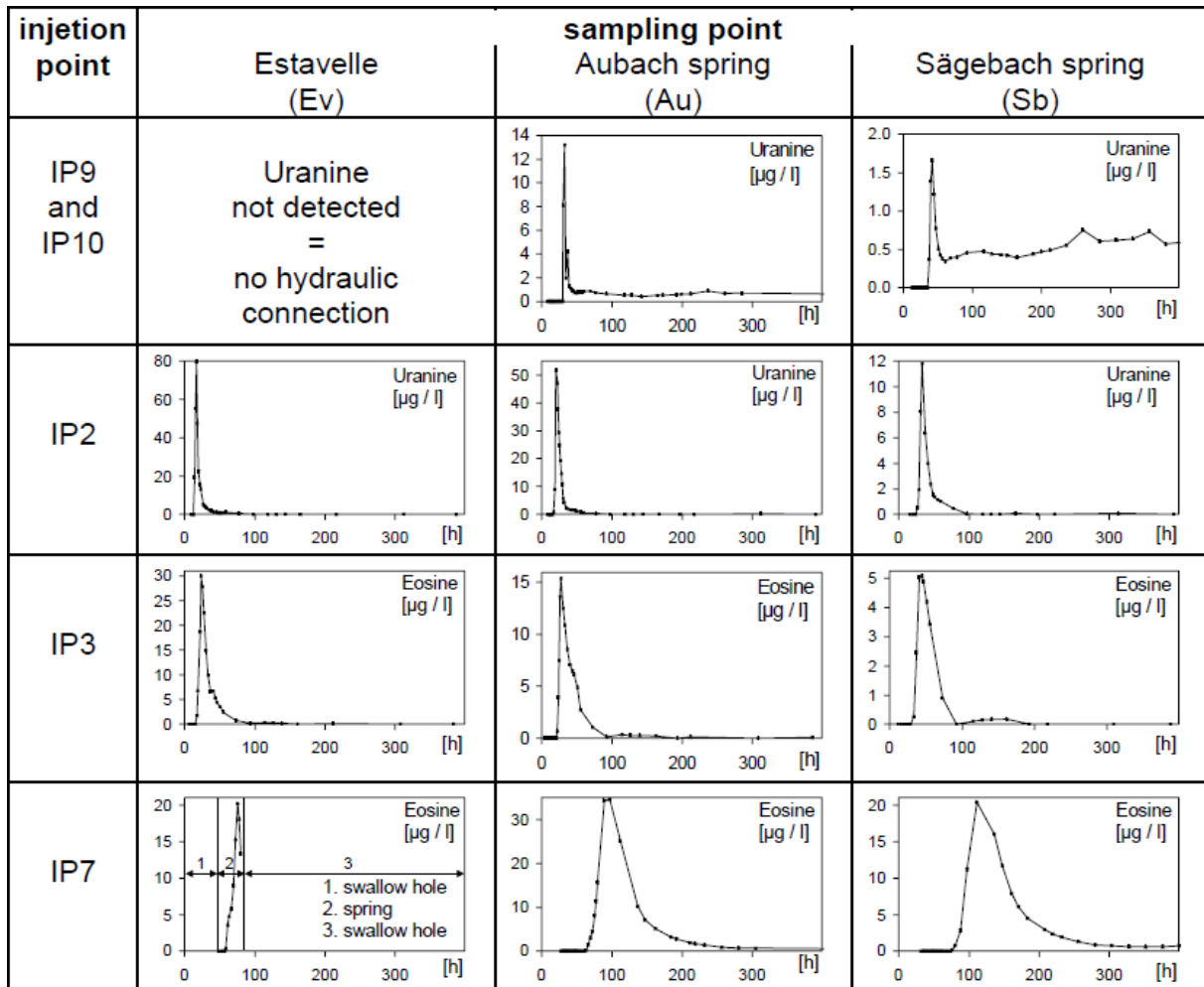


Fig. 6.7: Selected breakthrough curves from different tracer tests in the eastern part of the Hochifen-Gottesacker area (from Goldscheider, 2002).

The uranine that was injected in IP9 and IP10 reached Aubach Spring about 31 h after injection and later on the other 3 karst springs (Bü, Ks, Sb) in the Schwarzwasser valley. These results prove that the underground watershed is at least 100 m west of the culmination line. The uranine, which was injected in IP2 reached the Estavelle after 14 h and the between 17 and 27 h the four karst springs in the Schwarzwasser valley. Thus, the syncline III/IV belongs to the catchment of the Estavelle and the four springs. The eosine which was injected in IP3 reached the Estavelle and the four karst springs after 23 to 44 h. Eosine was also found in the Breitach river, at different concentrations, which is evidence that the bottom spring (Bo) also discharges water from the Schwarzwasser valley and is therefore the lowest outlet of the whole karst system. The injected eosine of IP7 reached the Estavelle and the four karst springs after 59 – 76 h. This tracer test proved the existence of a hydraulically connected karst aquifer in the entire valley which is discharged by the Estavelle, the four karst springs and the bottom spring. The uranine, which was injected under low water conditions in the Schwarzwasser cave (IP6) reached the karst springs after 7 - 22 h. The cave connects the surface river with the underground karst aquifer which is further downstream drained by the four karst springs. This and all other tracer tests from the eastern part of the Gottesacker area prove that the groundwater from the Schwarzwasser valley flows under the Mahdtal valley and rises up to the Sägebach Spring (Sb) which is located at the opposite side of the valley. Tracer tests from the Hölloch cave show that Sb spring gets additional inflow from the Mahdtal valley (Goepfert & Goldscheider, 2008). The tracers that were injected in an old sewage shaft and a neighboring karst shaft (IP4 and IP5). Reached the four karst springs in the

Schwarzwasser valley within a few days, proving that the waste that had been dumped into the cave is potentially endangering the water quality of the karst springs (Goldscheider, 2000).

The karst aquifer in the Hochifen-Gottesacker area is characterized by high flow velocities. An overview of the maximum and dominant flow velocities is given in the following table (modified after Goldscheider, 2002).

Table 6.1: Groundwater flow velocities in the eastern part of the Hochifen-Gottesacker area.

flow paths	Hydrologic conditions	example	max flow velocity [m/h]	dominant flow velocity [m/h]
through a large, open syncline	low – high	IP9 – Au	149	141
	moderate	IP2 – Bü	331	233
karst groundwater collector in the Schwarzwasser valley	low – high	IP7 – Sb	98	66
	moderate	IP3 – Au	160	143
	low	IP6 – Au	147	85
	low	IP6 – Sb	100	71
rock fall mass	low – high	IP8 – Ru	113	81

On the basis of geological and hydrogeological information, it is possible to delineate the catchments of the individual springs, which were proven by the tracer tests. In the following figure, the individual catchments of the springs from the eastern Hochifen-Gottesacker area are shown.

The eastern Hochifen-Gottesacker area forms a large, connected catchment. Under low-water conditions, when the Estavelle is a swallow hole, the catchment includes the Flysch mountains on the southeastern side of the Schwarzwasser valley (Goldscheider, 2002). The entire catchment can be subdivided into sub-catchments by the crests of the anticlines. Bo and Sb drain the entire catchment, Au, Bü and Ks drain the entire area without the Mahdtal valley and when the estavelle (Ev) acts as spring, it drains the Schwarzwasser valley upstream from the Estavelle and the southern part of the Gottesacker area (syncline III/IV, Fig. 6.8).

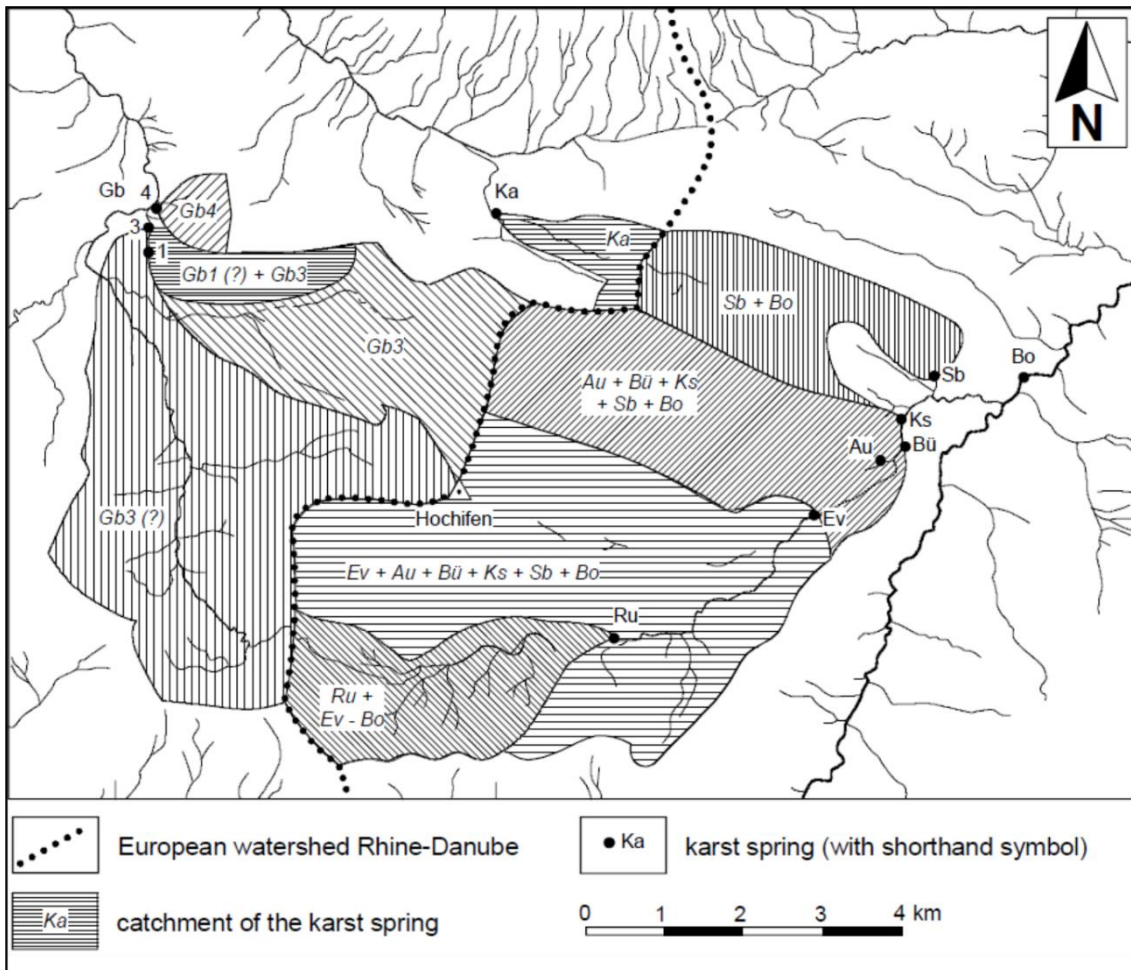


Fig. 6.8: Catchments of important springs in the eastern Hochifien-Gottesacker area (modified after Goldscheider, 2002).

6.3 Planned tracer tests

A combined tracer test was planned for the summer 2021, at the end of the snowmelt phase. A combination of soluble tracers, Uranine and Lithium Chloride, and a particle tracer was to be used. The aim was a comparison of the different tracers, for which this system is perfect, due to the knowledge from previous tracer tests. The previous results also allow to derive the perfect dosage of Uranine and Lithium Chloride for this test. Also the sampling can be planned beforehand, since the expected velocities and durations are well known.

The particle tracer was gained from fine-grained sediments in the Schwarzwasser valley, close to the swallow holes. Results of certain particle size classes allow conclusions on the potential transport of fecal indicator bacteria (*E. coli*). For the use of particle tracers, it is essential to know the natural background for the different size classes. Rainfall or snowmelt, but also human activities like excavations, can have a strong influence on the particle load and also lead to daily variabilities. To match this requirement, a long-term monitoring was already started at Aubach and Sägebach spring, leading to a better knowledge of the dynamic for the different particle size classes during the phase of intensive snowmelt.

Due to the hydrological conditions in spring and summer 2021, the Estavelle never acted as a swallow hole, but as spring during the whole period, the combined tracer test could not be conducted until now. Depending on the development of the hydrological conditions, the tracer test could be performed at a later point of time.

6.4 Innovative Modeling

The first tests of the new CTRW approach with kilometer-scale field data and also the first application to data from a karst aquifer, was made using results from tracer tests in the Hochfifen-Gottesacker system (Goeppert et al., 2020). Fig. 6.9 shows the results of CTRW compared to the conventional ADM and 2RNE models. For both springs, Aubach and Sägebach spring, it is clearly visible that ADM and 2RNE models can reproduce the peak of all breakthrough curves (Fig. 6.9), but are not able to fit the lower concentrations. However, the innovative CTRW is capable of taking the long tailing into account and shows the best fit for all breakthrough curves in this karst system, making it an important modeling tool for low concentrations and long travel times (Goeppert et al., 2020).

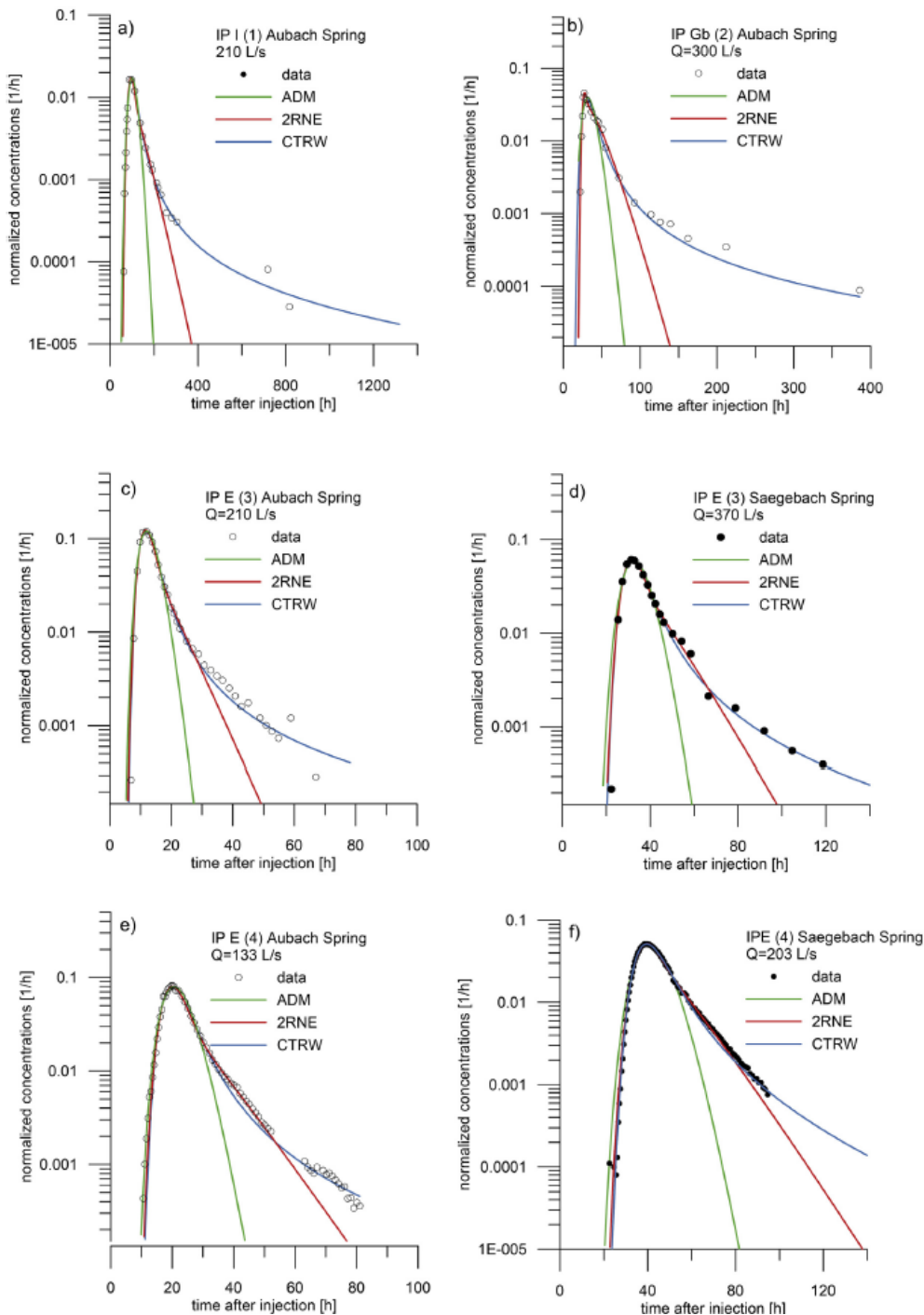


Fig. 6.9: Six breakthrough curves from Aubach and Sägebach spring modeled using ADM, 2RNE, and CTRW models. The new CTRW approach shows the best fit for the tailing of all curves.

6.5 References

Goeppert, N., Goldscheider, N. (2008) Solute and Colloid Transport in Karst Conduits under Low- and High-Flow Conditions, *Groundwater*, 46, 1, 61-68.

Goldscheider, N. (1998) Der Ladstattschacht - tracerhydrologische Untersuchungen einer organischen Altlast im alpinen Karst. *Schr. Angew. Geol. Karlsruhe*, 50: 155-172, Karlsruhe.

Goeppert, N., Goldscheider, N., Berkowitz, B. (2020) Experimental and modelling evidence of kilometer-scale anomalous tracer transport in an alpine karst aquifer, *Water Research*, 178.

Goldscheider, N. (2002) Hydrogeology and Vulnerability of Karst Systems - Examples from the Northern Alps and the Swabian Alp, *Schr. Angew. Geol. Karlsruhe*, 68, 263 S., Karlsruhe.

Goldscheider, N. (2005) Fold structure and underground drainage pattern in the alpine karst system Hochifen - Gottesacker, *Eclogae geol. Helv.*, 98, 1-17.

7. Unica springs catchment (Slovenia)

7.1 Field site description

The Unica springs are located in southwestern Slovenia (Fig. 7.1), which occupies the northern part of the Dinaric Karst, the largest continuous karst area in Europe, stretching along the Adriatic Coast. Two larger permanent springs emerge on the edge of a karst polje: Unica and Malenščica that join into the Unica River. The Malenščica is a regionally important drinking water source (Petrič 2010), which drains diffusely with discharges from 1.1 to 11.2 m³/s. The Unica emerges through a network of large underground channels with common discharges ranging from 0.2 to 74.8 m³/s. Two underground river channels (branches of the Rak and Pivka) converge underground. Part of the cave network includes a large Postojna-Planina Cave System, known worldwide for its rich biodiversity (Culver & Pipan 2013).

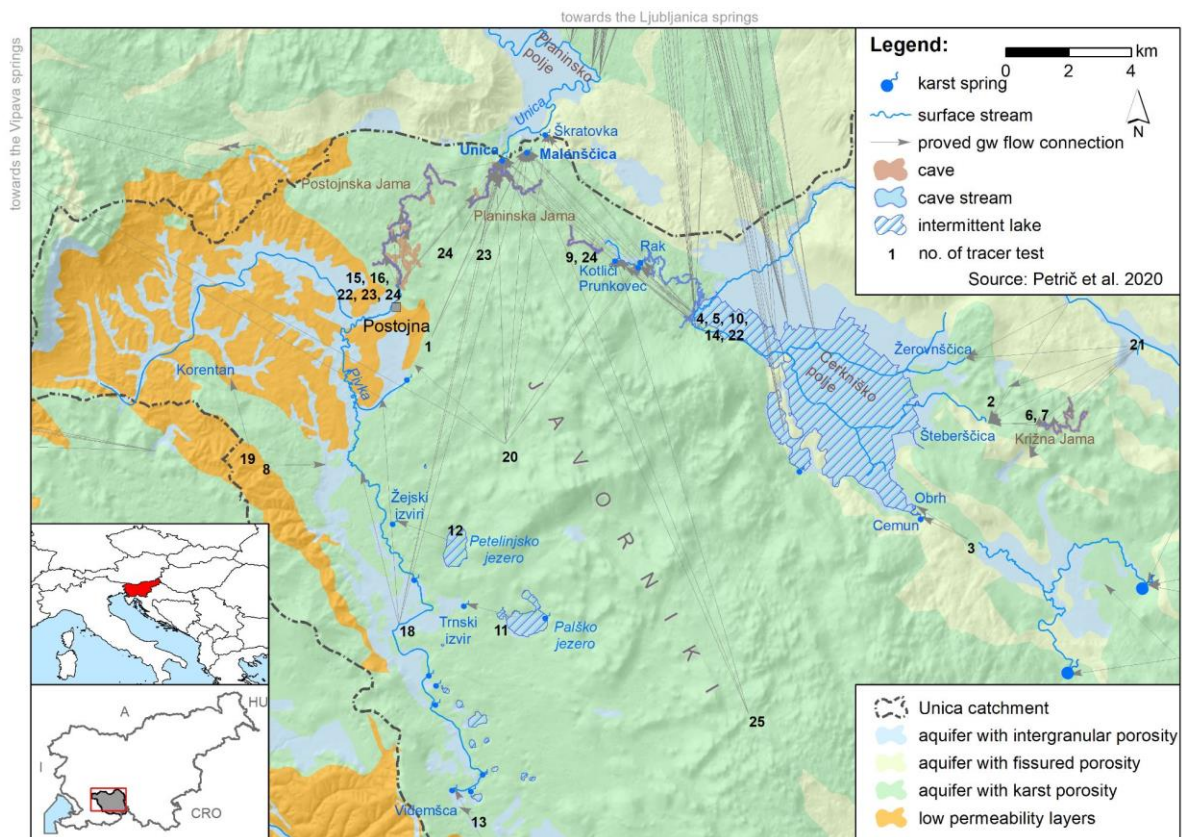


Fig. 7.1: Hydrogeological situation of the study area with proven groundwater flow connections.

The springs drain a complex binary aquifer system that extends over an area of about 820 km² and consisting of three distinct recharge areas: autogenic recharge from the extensive karst aquifer of the Javorniki Massif, allogenic recharge from Pivka River Basin to the west, and a chain of karst poljes to the east of the massif. The predominant lithology of the karst aquifer is Cretaceous rocks, mainly limestones, which in places change to dolomites and breccias. To a lesser extent, Jurassic and Paleogene carbonate rocks also occur. The northern part of the Pivka Basin consists of poorly permeable Eocene flysch, which conditions a superficial river network. In a narrow belt extending along the poljes, Upper Triassic dolomites predominate, changing to Jurassic limestones and dolomites in the south and west. These rocks form aquifers with fracture porosity, which in places have very poor to moderate permeability, and in some parts a superficial river network is developed. As the karst poljes follow each other in a row downgradient, the same water sinks and reappears several times.

The alluvial sediments at the bottoms of the poljes and river valleys are of Quaternary age. They form smaller aquifers with intergranular porosity.

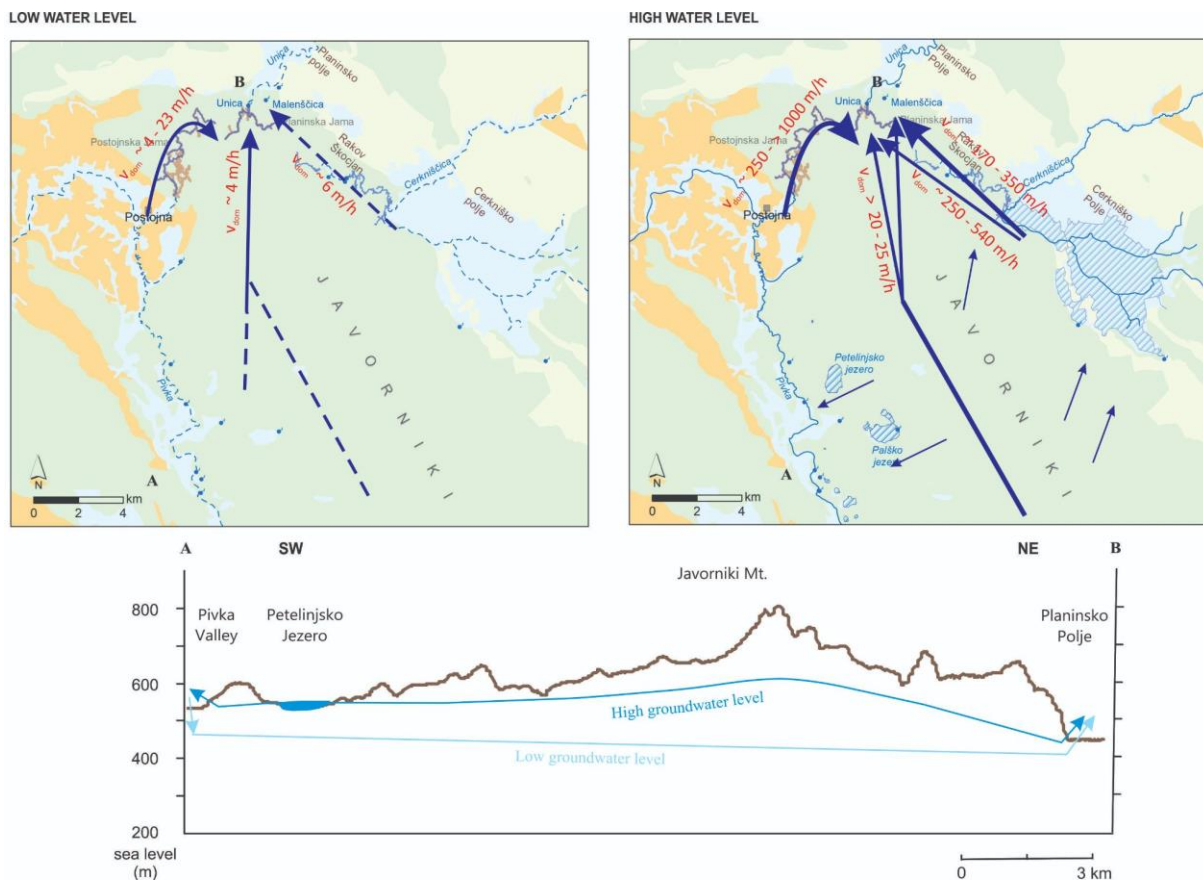


Fig. 7.2: Schematic presentation of groundwater flow variability in the study area under different hydrological conditions (modified after Ravbar 2013, Petrič et al. 2020).

The area is considered pioneering for speleological and karstological research and belongs to the so-called Classical Karst area. The springs studied are located at an altitude of about 550 m above sea level and the peaks of the karst massif reach an altitude of 1,800 m above sea level. Climatologically, the area is located in a transition zone between Cfb and Dfb subtypes according to the Köppen-Geiger climate classification, with a mean annual precipitation (1991-2020, Postojna meteorological station) of 1,520 mm and a mean annual air temperature of 9.8°C (Jan 0.6°C, Jul 19.5°C; ARSO 2021a). Pronounced hydrological variability characterises the area, with groundwater level fluctuations of the order of tens of metres within a short period of time, leading to variations in flow velocities and directions and surface-groundwater interactions (Fig. 7.2; Ravbar 2013).

7.2 Tracer tests database

To date, various geological, geomorphological, speleological and hydrological surveys have been carried out, including several tracer tests (Petrič et al. 2020). Their main purposes were to record groundwater flow directions and velocities, delineate the catchment area and protection zones, and improve groundwater tracing techniques (Kogovšek & Petrič 2004). Groundwater tracing also proved flow bifurcations, which suggest the area belongs to the Adriatic-Black Sea watershed (Kogovšek et al. 1999). Recently, artificial tracers have been used for several other purposes, such as to study the effects of different land use patterns on water source quality (Kogovšek et al. 2008), the dynamics of

prevailing water flow through the vadose zone (Petrič et al. 2018), the relationships between artificial and natural tracers (Ravbar et al. 2012), and to study karst vulnerability (Gabrovšek et al. 2010).

The tracer test database created as part of the KARMA project includes tracer tests conducted after 1954, when continuous discharge data were measured at major springs in the region (ARSO 2021b). Tracer tests that exclusively examined percolation through the vadose zone with sampling points within caves were excluded.

A total of 25 tracer tests were identified. Most of them were conducted in the 60's of the 20th century and in the first decade of the present century. In the majority of the tests, one type of tracer was injected at one site. Four tracer tests were performed with two or three injection sites and one test used multiple tracers. Uranine was used in 71% of the injection points, and NaCl, spore naphthionate and sulforhdamine G were used in the rest. In 77% of the cases, the injection point was a swallow hole, and in the remaining cases shafts, crevices or cave streams. In one case, a highway oil collector was used as the injection point. The amount of tracer used depended on the tracer type, hydrological conditions, injection mode, and discharges of the targeted springs.

Six tracer tests were conducted at high water conditions, two at high to moderate water conditions, nine at moderate water conditions, and four at low water conditions. During one tracer test, water conditions changed from low to medium and no such information could be retrieved for three tracer tests. Most of the injection sites were within 10 km of the sampling location, and the most distant was nearly 25 km away. Sampling sites were generally springs and cave streams, and in rare cases surface streams and boreholes. Considering linear distance, maximum flow velocities range from 3.8 to 750 m/h and peak flow velocities up to 1127 m/h. Such high velocities are achieved by flow of sinking streams through well-developed channels toward large springs. For the same section of groundwater flow, flow velocities may be several degrees lower at low water levels than at high water levels.

7.3 References

ARSO 2021a: Slovenian Environment Agency, Interactive weather. [Online] Available from: <https://meteo.arso.gov.si/met/en/app/webmet/> [Accessed 14th May 2021].

ARSO 2021b: Slovenian Environment Agency, Archive hydrological data. [Online] Available from: http://vode.arso.gov.si/hidarhiv/pov_arhiv_tab.php [Accessed 5th May 2021].

Culver, D.C.; Pipan, T., 2013: Subterranean ecosystems. In: Encyclopedia of Biodiversity, 2nd ed.; Levin, S.A., Ed.; Academic Press: Waltham, Massachusetts, USA, 2013; pp. 49–62, ISBN 978-0-123-84719-5.

Gabrovšek, F., Kogovšek, J., Kovačič, G., Petrič, M., Ravbar, N., Turk, J., 2010: Recent results of tracer tests in the catchment of the Unica River (SW Slovenia). *Acta carsologica*, 39/1, 27-37. <https://doi.org/10.3986/ac.v39i1.110>

Kogovšek, J., Petrič, M., 2004: Advantages of longer-term tracing - three case studies from Slovenia. *Environmental geology*, 47, 76-83. <https://doi.org/10.1007/s00254-004-1135-8>

Kogovšek, J., Knez, M., Mihevc, A., Petrič, M., Slabe, T., Šebela, S., 1999: Military training area in Kras (Slovenia). *Environmental Geology*, 38, 1, 69-76.

Kogovšek, J., M. Prelovšek, Petrič, M., 2008: Underground water flow between Bloke plateau and Cerknica polje and hydrologic function of Križna jama, Slovenia. *Acta carsologica*, 37/2-3, 213-225. <https://doi.org/10.3986/ac.v37i2-3.147>

Petrič, M., 2010: Characterisation, exploitation, and protection of the Malenščica karst spring, Slovenia.- In: Kresic, N. & Z. Stevanovic (eds.) *Groundwater Hydrology of Springs. Engineering, Theory, Management and Sustainability*. Butterworth-Heinemann, pp. 428-441, Burlington.

Petrič, M., Kogovšek, J., Ravbar, N., 2018: Effects of the vadose zone on groundwater flow and solute transport characteristics in mountainous karst aquifers—the case of the Javorniki–Snežnik massif (SW Slovenia). *Acta Carsologica*, 47(1), 35-51. <https://doi.org/10.3986/ac.v47i1.5144>

Petrič, M., Ravbar, N., Gostinčar, P., Krsnik, P., Gacin, M., 2020: GIS database of groundwater flow characteristics in carbonate aquifers: Tracer test inventory from Slovenian karst. *Applied Geography*, 118, 102191. <https://doi.org/10.1016/j.apgeog.2020.102191>

Ravbar, N., Barbera, J. A., Petrič, M., Kogovšek, J., Andreo Navarro, B., 2012: The study of hydrodynamic behaviour of a complex karst system under low-flow conditions using natural and artificial tracers (the catchment of the Unica River, SW Slovenia). *Environmental earth sciences*, 65/8: 2259-2272. <https://doi.org/10.1007/s12665-012-1523-4>

Ravbar, N., 2013: Variability of groundwater flow and transport processes in karst under different hydrologic conditions. *Acta Carsologica*, 42(2-3), 327–338. <https://doi.org/10.3986/ac.v42i2.644>

8. Conclusions and outlook

8.1 General characteristics

A total of 111 tracer tests, with 238 documented breakthrough curves, were conducted in the KARMA test sites, mostly using fluorescence dyes. With five different test sites, various injection and sampling points and varying hydrological conditions, these tests cover a wide range of different settings and situations. Fig. 8.1 (left) shows the distribution of linear distances between injection points and sampling points for all recorded breakthroughs. While the majority of all distances are between 2500 and 7000 m, two tests in the Unica catchment and one test in the Lez catchment covered distances of more than 20 km. The shortest distance, 90 m, was also a test in the Unica catchment. Also all calculated maximum velocities (middle) and peak velocities (right) are displayed in Fig. 8.1. Amongst others, the degree of karstification is one parameter that flow velocities depend on. Most calculated velocities are between 50 and 200 m/h and almost all outliers derive from tracer tests in the Qachqouch catchment.

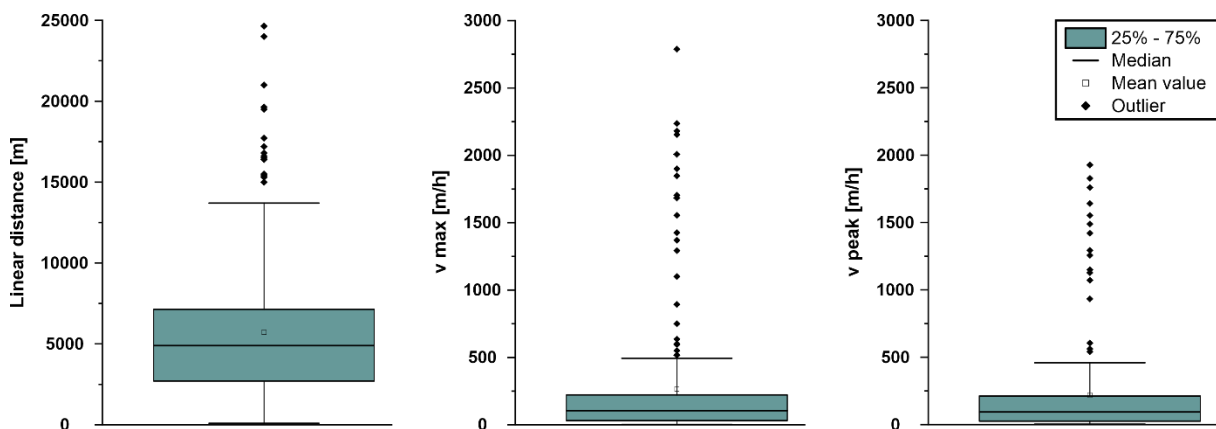


Fig. 8.1: Overview of the variety of linear distances between injection and sampling points, as well as maximum and peak velocities.

135 out of the 238 breakthroughs have a known cave between injection and sampling point (Fig. 8.2, left). In this case, known cave systems relate to registered and accessible cave systems. Connections without a known cave system can also include highly karstified zones or even small caves with high flow velocities, but are just not registered or investigated. As expected, flow through a cave stream increases the velocities significantly (Fig. 8.2, right). Especially the tracer tests in the Jeita cave in Lebanon showed a very fast flow and accounts for all values over 1000 m/h. Most connections with cave show maximum velocities between 40 and 500 m/h and peak velocities between 30 and 400 m/h. For connections without cave, v_{max} is between 25 and 70 m/h and v_{peak} between 20 and 60 m/h.

Additionally, velocities for tracer tests without information about caves are shown in Fig. 8.2 (right). One of these tests, from Lebanon, shows the overall highest calculated velocity with 2788 m/h. In order to reach such a fast flow, a high degree of karstification or a large conduit, as well as a high hydraulic gradient, is needed. Also two other tests show velocities of more than 500 m/h, indicate highly karstified flow paths.

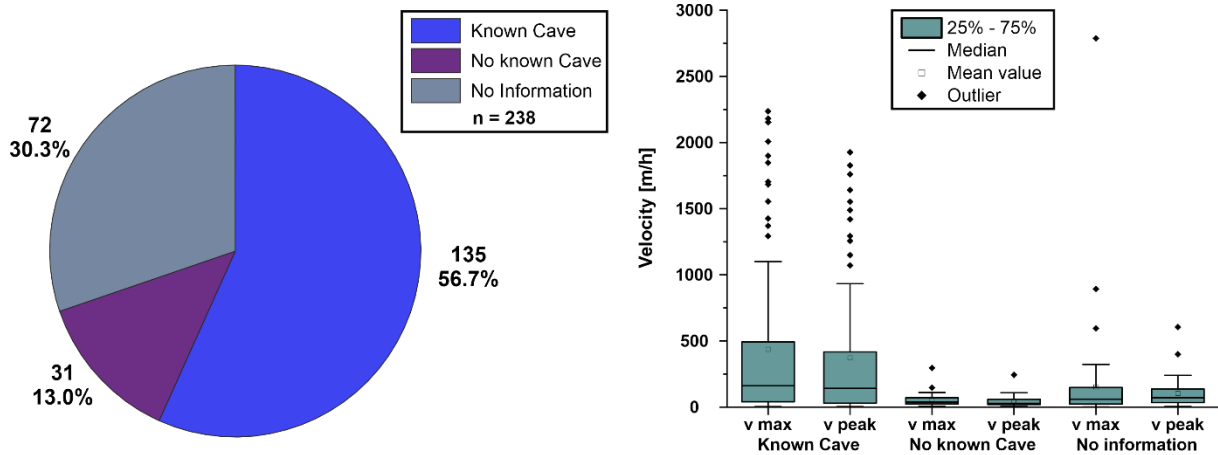


Fig. 8.2: Left: Percentages and absolute values of breakthroughs with and without a known cave system between injection and sampling point. Right: Comparison of velocities from tracer tests with flow through a known cave to flow velocities without a known cave and tracer tests without information about caves.

8.2 Comparison of descriptive transport parameters

The tracer test in the KARMA test sites show a wide range of distances and flow velocities. Fig. 8.3 shows the variety of distances and velocities for the respective test sites. While the longest linear distances were covered by tests in the Unica catchment (No. 2, Slovenia) and the Lez catchment (No. 4, France). The by far highest velocities were recorded in the Qachqouch catchment, most of them due to the fast flow through the Jeita cave.

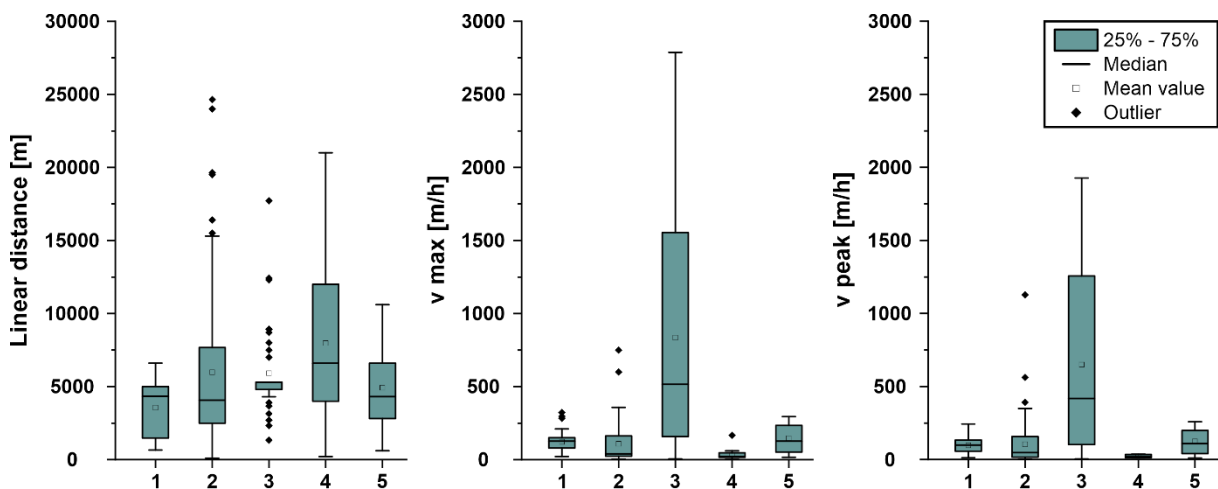


Fig. 8.3: Distribution of linear distances, maximum velocities and peak velocities for each KARMA test site (1 = Hochifen-Gottesacker, Germany/Austria; 2 = Unica catchment, Slovenia; 3 = Qachqouch catchment, Lebanon; 4 = Lez catchment, France; 5 = Province Málaga, Spain).

Fig. 8.4 (left) displays maximum velocities and linear distances of all recorded tracer breakthroughs in the KARMA test sites. Since every test site has its own unique and complex karst system, no test-site-crossing conclusions can be drawn. Fig. 8.4 (right) shows the relation between discharge and maximum velocity, which confirms that every system differs and reacts differently. Repeated tracer tests in the Jeita cave in Lebanon document an almost linear relationship between discharge and maximum velocity for this connection. For one connection in the Unica test site, Pivka ponor – Otoška jama, a six times higher discharge (810 L/s and 5100 L/s) led to an almost 19-fold increased peak velocity (60 m/h compared to 1127 m/h). However, smaller changes in discharge can also lead to remarkable changes of flow velocities, e.g. the connection Mala Karlovica – Kotliči in the Unica test site. There, a 30 % increase in discharge (7200 L/s to 9260 L/s) led to a doubled v max (125 m/h to 296 m/h).

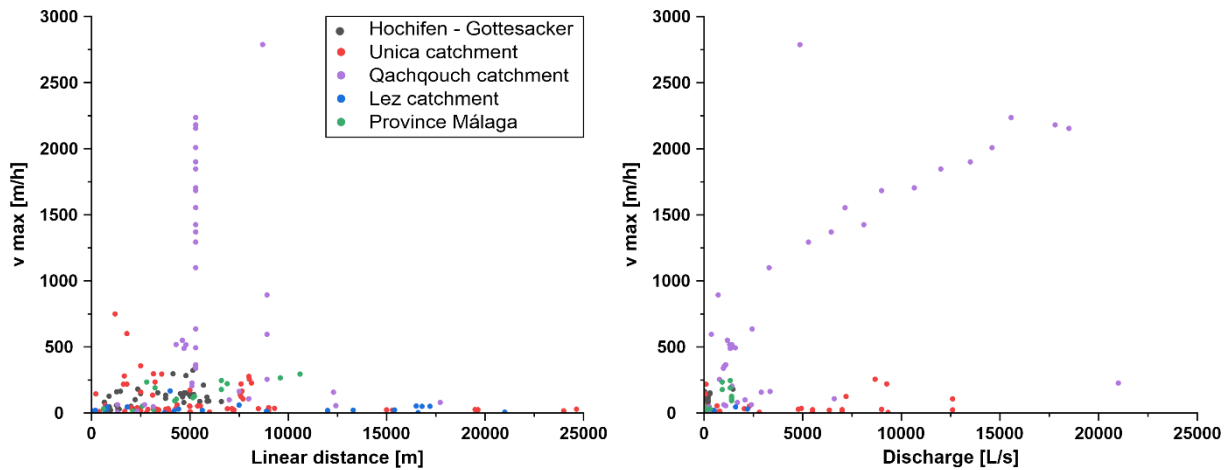


Fig. 8.4: Left: Maximum velocity versus linear distances of all recorded tracer breakthroughs in the KARMA test sites. Right: Maximum velocity versus spring discharge for all recorded tracer breakthroughs in the KARMA test sites.

8.3 Impact of hydrological conditions

An important factor influencing the transport parameters are the hydrological conditions during the test period. Due to higher pressures and gradients, high flow conditions lead to higher velocities. Also the tracer tests in the KARMA test sites underline this correlation (Fig. 8.5). However, depending on the system and the degree of karstification, velocities can also be very low during high flow conditions.

Mean flow and low flow conditions lead to less variation for v_{max} and v_{peak} as opposed to high flow conditions. Mean flow also results in higher median values for v_{max} and v_{peak} as opposed to low flow conditions. The outliers for v_{max} and v_{peak} during mean flow and the highest values during low flow conditions are from tests in the Jeita cave in Lebanon. This test site shows the highest velocities for all conditions, except for the maximum velocity of 2788 m/h, which also originates from a test in the Qachqouch catchment.

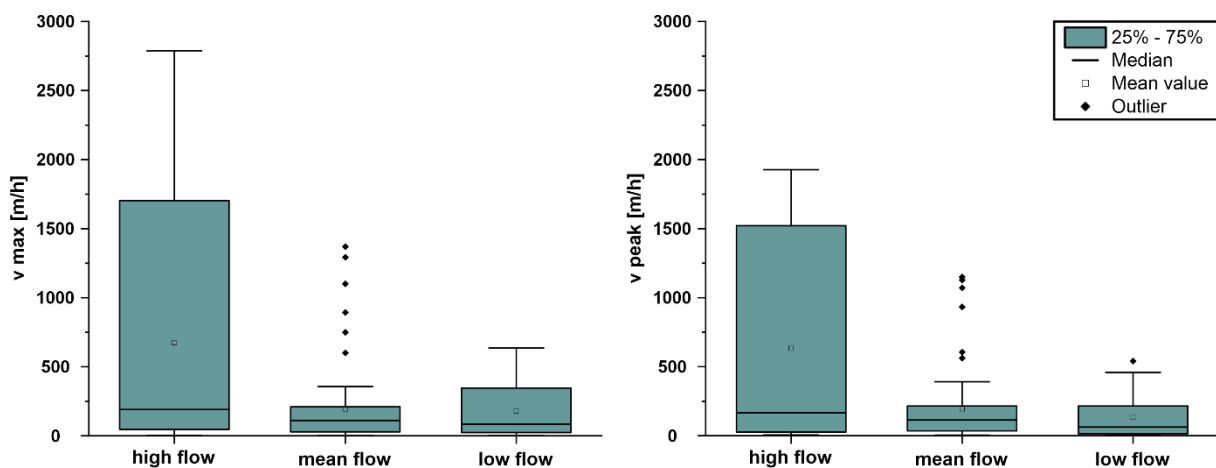


Fig. 8.5: Maximum (left) and peak velocities (right) for all tracer tests in the KARMA test sites depending on the hydrological conditions during the test period.

8.4 Tracer tests as tools for vulnerability assessment

Tracer tests can be used to validate a groundwater vulnerability assessment, as they allow observing the transit time and concentration decline of a potential contaminant from the injection point (origin) to a sampling point (target) (Andreo et al., 2006). While conservative tracers can be used to validate intrinsic vulnerability, reactive tracers allow validating specific vulnerability. If a tracer breakthrough

curve is available at the monitoring point, the validation of a point vulnerability map is possible. Tracer tests can be used to validate at certain points only, while large surfaces cannot be validated with this method (Goldscheider et al., 2001).

Spring hydrographs and natural tracers can also be used to validate a vulnerability assessment. In contrast to artificial tracer tests, these methods cannot be used to check the vulnerability at specific points, but provide information on the response of the whole aquifer system on external impacts. Fast and marked hydraulic, hydrochemical and isotopic reactions on hydrologic events indicate a high vulnerability of the aquifer (Bakalowicz, 2004; Andreo et al., 2006).

In the framework of the KARMA project it is also planned to validate generated vulnerability maps in the different test sites with tracer tests.

8.5 References

Andreo, B., Goldscheider, N., Vadillo, I., Vias, J.M., Neukum, C., Sinreich, M., Jimenez, P., Brechenmacher, J., Carrasco, F., Hötzl, H., Perles, J.M., Zwahlen, F. (2006) Karst groundwater protection: First application of a Pan-European Approach to vulnerability, hazard and risk mapping in the Sierra de Libar (Southern Spain), *Science of the Total Environment*, 357, 1-3, 54-73.

Bakalowicz, M. (2004) Hydraulics and spring hydrographs. In: Zwahlen, F. (editor) *Vulnerability and risk mapping for the protection of carbonate (karst) aquifers*, EUR 20912, Brussels, European Commission, Directorate-General XII Science, Research and Development, 132.

Goldscheider, N., Hötzl, H., Fries, W., Jordan, P. (2001) Validation of a vulnerability map (EPIK) with tracer tests. In: Mudry, J., Zwahlen, F., *Seventh conference on limestone hydrology and fissured media*, (Sci Tech Environ Mém), 20–22 September 2001, Besancon, France, 167– 170.